AD-A169 159 SEARCH FOR FAR INFRARED RADIATION FROM OPTICALLY AND ACOUSTICALLY PUMPED.. (U) CORNELL UNIV ITHACA NY LAB OF ATOMIC AND SOLID STATE PHYSICS.. A J SIEVERS 15 APR 86 1/1

UNCLASSIFIED ARO-19793.4-PH DAAG29-83-K-0044 F/G 20/5 NL

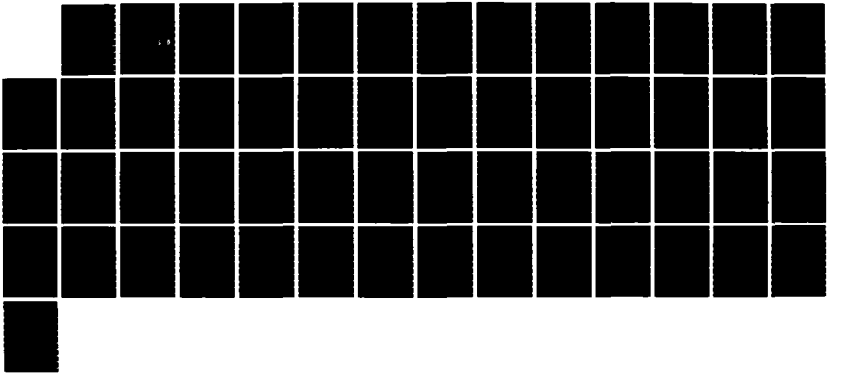

1.0
1.1
1.25
1.4
1.6
2.8
3.2
3.6
4.0
2.2
2.0
1.8

(2)

UNCLASSIFIED
SECURITY CLASSIFICATION OF THIS PAGE (When Data Entered)

REPORT DOCUMENTATION PAGE

READ INSTRUCTIONS BEFORE COMPLETING FORM

1. REPORT NUMBER: ARO 19793.4-PH
2. GOVT ACCESSION NO.
3. RECIPIENT'S CATALOG NUMBER

4. TITLE (and Subtitle): Search for Far Infrared Radiation from Optically and Acoustically Pumped Defect Modes
5. TYPE OF REPORT & PERIOD COVERED: Final Report 14 Feb 83 - 13 Feb 86
6. PERFORMING ORG. REPORT NUMBER

7. AUTHOR(s): A. J. Sievers, Prof. of Physics
8. CONTRACT OR GRANT NUMBER(s): DAAG 29-83-K-0044

9. PERFORMING ORGANIZATION NAME AND ADDRESS:
LASSP
Cornell University
Ithaca, NY 14853-2501
10. PROGRAM ELEMENT, PROJECT, TASK AREA & WORK UNIT NUMBERS

11. CONTROLLING OFFICE NAME AND ADDRESS:
U. S. Army Research Office
Post Office Box 12211
Research Triangle Park, NC 27709
12. REPORT DATE: Apr. 15, 1986
13. NUMBER OF PAGES: 51

14. MONITORING AGENCY NAME & ADDRESS (if different from Controlling Office):
P. A. Curtiss
123 Day Hall
Ithaca, NY 14853
15. SECURITY CLASS. (of this report): Unclassified
15a. DECLASSIFICATION/DOWNGRADING SCHEDULE

16. DISTRIBUTION STATEMENT (of this Report)

Approved for public release; distribution unlimited.

17. DISTRIBUTION STATEMENT (of the abstract entered in Block 20, if different from Report)

NA

18. SUPPLEMENTARY NOTES

The view, opinions, and/or findings contained in this report are those of the author(s) and should not be construed as an official Department of the Army position, policy, or decision, unless so designated by other documentation.

19. KEY WORDS (Continue on reverse side if necessary and identify by block number)

lattice impurity modes -- elastic instability - far infrared transmission measurements, molecular vibrations in crystals, ultrasonic studies of persistent holes -- Vibrational defects which hole burn and show vibrational fluorescence -- solid state IR vibrational lasers

20. ABSTRACT (Continue on reverse side if necessary and identify by block number)

More than one elastic ground state configuration has been found for both monatomic and polyatomic defects matrix isolated in alkali halide crystals. Multiple ground states give rise to persistent changes in the vibrational absorption spectrum of molecules when the internal vibrational modes of the defect are excited with a high resolution but tunable IR laser. The end result is that spectral holes with a width characteristic of the dephasing time of the vibrational mode can be created in the inhomogeneously strain broadened spectrum.

cont.

DD FORM 1 JAN 73 1473 EDITION OF 1 NOV 65 IS OBSOLETE

UNCLASSIFIED
SECURITY CLASSIFICATION OF THIS PAGE (When Data Entered)

The technique has been used to identify $CN^-:Na^+$, a new kind of vibrational defect which hole burns and also shows vibrational fluorescence in the IR. The discovery of the first solid state IR vibrational laser was a direct consequence of these kinds of measurements. The observations of transient and persistent hole burning, of vibrational fluorescence and of vibrational laser radiation demonstrate that diatomic molecules are more weakly coupled to the lattice than are polyatomics.

Search for Far Infrared Radiation from Optically and Acoustically Pumped Defect Modes

FINAL REPORT

A. J. Sievers

April 15, 1986

U. S. ARMY RESEARCH OFFICE

DAAG 29-83-K-0044

CORNELL UNIVERSITY

Table of Contents

1. ABSTRACT

More than one elastic ground state configuration has been found for both monatomic and polyatomic defects matrix isolated in alkali halide crystals. Multiple ground states give rise to persistent changes in the vibrational absorption spectrum of molecules when the internal vibrational modes of the defect are excited with a high resolution but tunable IR laser. The end result is that spectral holes with a width characteristic of the dephasing time of the vibrational mode can be created in the inhomogeneously strain broadened spectrum.

The technique has been used to identify $CN^-:Na^+$, a new kind of vibrational defect which hole burns and also shows vibrational fluorescence in the IR. The discovery of the first solid state IR vibrational laser was a direct consequence of these kinds of measurements. The observations of transient and persistent hole burning, of vibrational fluorescence and of vibrational laser radiation demonstrate that diatomic molecules are more weakly coupled to the lattice than are polyatomics.

2. PROGRESS REPORT

2.1 Introduction

Our three year program to study the vibrational responses of matrix isolated molecules which have been illuminated with high intensity laser radiation has produced new and unexpected results of both a fundamental and applied nature. In general these experiments support the original premise of this program, namely, that far infrared radiation may be obtainable from optically pumped defect modes. All of our high intensity and high resolution work to date has been directed towards identifying the appropriate lattice-defect system. Because we are the first group to use these IR techniques to probe defect modes it is perhaps not surprising that once we realized the inability of lattice defect theory to account for our experimental data a rash of new discoveries have occurred. This proposal describes a program which will follow a subset of these new findings so that we may learn more about defect mode relaxation in the far infrared part of the spectrum.

The observation of persistent spectral hole and antihole burning in the vibrational mode of ReO_4^- in alkali halide crystals demonstrated for the first time that for matrix isolated molecules such effects could be produced. The effect for the spherical top molecule was traced back and connected with the two equivalent positions or configurations available to a tetrahedral defect in a cubic lattice site.

The search for the boundary between lattice-defect systems which have more than one ground state configuration and those that have only one, led us to discover that even a substitutional point defect in a cubic lattice produces more than one low lying elastic configuration. This work is described in Sec. 2.2. The results are of fundamental importance since it may be that

an entire spectrum of these elastic states occurs for many different kinds of defect systems. In this case more degrees of freedom are available at low energies than previously determined from lattice-defect theories.

At the same time that these new elastic states for point defects were being identified, our measurements on the nonlinear properties of molecular vibrational modes intensified. Some of these results are described in Sec. 2.3.

The discovery of the persistent antihole and the ultrasonic modulation of both persistent holes and antiholes for the ReO_4^- molecule not only helped us identify the actual lattice-defect dynamics of the formation of persistent features but also showed us that these effects could be used as a sensitive and nonbonding ultrasonic wave detector.

Measurements on other spherical top molecules have demonstrated that Fermi resonances, which often occur between internal modes of a complex molecule, can completely eliminate high power IR bleaching which is a characteristic feature of the ReO_4^- vibrational mode.

Linear molecules such as CN^-, which were expected to be simple, show a very complex dynamical behavior. For example, $KBr:CN^-:Na^+$ produces a new kind of vibrational center which shows both vibrational fluorescence and persistent hole burning. The fluorescent lifetime is on the order of 40 msec and the persistent holes are stable up to 45°K. We have found that the hole burning process is spectrally very different from the spherical top molecule case. A new high resolution spectroscopic technique, which makes use of a diode laser in conjunction with an F.F.T. interferometer, has played an important role in increasing our understanding of this defect system.

Our investigation of the interaction between CN^- molecules at high concentrations has lead to the identification of resonant vibration-vibration hopping as the important energy transfer process. Once this effect was understood it was possible to design a KBr:CN^- system to lase in the 5 μm wavelength region. This first solid state vibrational laser was demonstrated in pulse operation in 1984 and in CW operation in 1985.

During the past three years twenty seven publications and three theses, two Ph.D.'s and one Masters, have resulted from this program.

2.2 Lattice Impurity Modes

2.2.1. Elastic Instability for Ag^+ in KI

Unexpected temperature dependences are observed in the far infrared absorption spectrum of Ag^+ in KI. The low temperature impurity induced vibrational absorption lines decrease in strength and new features with different characteristic frequencies grow as the temperature is increased from 1.2 to 10 K. The dominant component in the high temperature spectrum is non-resonant absorption. It produces a contribution to the real part of the dielectric function which can be monitored with increased precision with a radio frequency capacitance bridge. To account for both kinds of experimental data we have found that, in addition to the ground state arrangement of the point defect-lattice system, a second elastic configuration must be nearby in energy.

The Ag^+ impurity induced spectrum in KI was for many years characterized by a sharp absorption line[1] at 17.3 cm^{-1}. Studies of the behavior of this mode under uniaxial stress, electric field and hydrostatic pressure have shown that at low temperatures the Ag^+ ion behaves as a substitutional impurity at a normal lattice site, i.e. the impurity does not exhibit displacive tunneling around the normal lattice site nor is it frozen in an offcenter position[1].

In 1971, Kirby[2] showed that the complete low temperature far infrared spectrum has many more features. In addition to the T_{1u} resonant mode at 17.3 cm^{-1} there exists an E_g+T_{1u} combination band at 29.8 cm^{-1}, an $A_{1g}+T_{1u}$ combination band at 44.4 cm^{-1}, two density of states peaks at 55.9 and 63.6 cm^{-1} and finally the T_{1u} localized gap mode at 86.2 cm^{-1}. In addition to these infrared active modes, Kirby also identified two even

resonant modes of A_{1g} and Eg symmetry at 25 cm^{-1} and 16.35 cm^{-1}, respectively.

With increasing temperature the strengths of all of the ir active features, including the combination bands decrease. The gap and resonant modes show identical temperature dependences, both disappearing at a temperature slightly above 20 K. At the same time nonresonant absorption appears at low frequencies and two lines develop[3] at 69 cm^{-1} and 78.5 cm^{-1}.

The characteristic temperature dependent features in the low frequency region are shown in Fig. 1 where the difference between the absorption coefficient at the temperatures shown and that at 20.6 K is plotted versus temperature. Since the nonresonant absorption is not present at 1.2 K and the resonant mode absorption is essentially gone by 20.6 K, the lowest spectrum in Fig. 1, α(1.2 K)- α(20.6 K), shows both components fully developed.

We have also measured the temperature dependence of the non-resonant absorption at a frequency far removed from the resonant mode region. A broad-band millimeter wave spectrum with an intensity maximum centered at 4 cm^{-1} and a full width at one half peak height of 4 cm^{-1} was used to measure the non-resonant absorption vs temperature growth curve. The experimental results normalized to the high temperature data are represented by the solid line shown in Fig. 2 (the ordinate for this trace is on the right).

In the classical Debye relaxation approximation when the thermal energy is much larger than the reorientational energy level spacings, the impurity induced dielectric response at frequency ω, is

$$\Delta_1 + i\Delta_2 = \Delta_0(1-i\omega\tau)^{-1} \qquad (1)$$

$$\text{where } \Delta_0 = 4\pi N \left(\frac{p^2}{3kT}\right) \left(\frac{\varepsilon_o + 2}{3}\right)^2 \qquad (2)$$

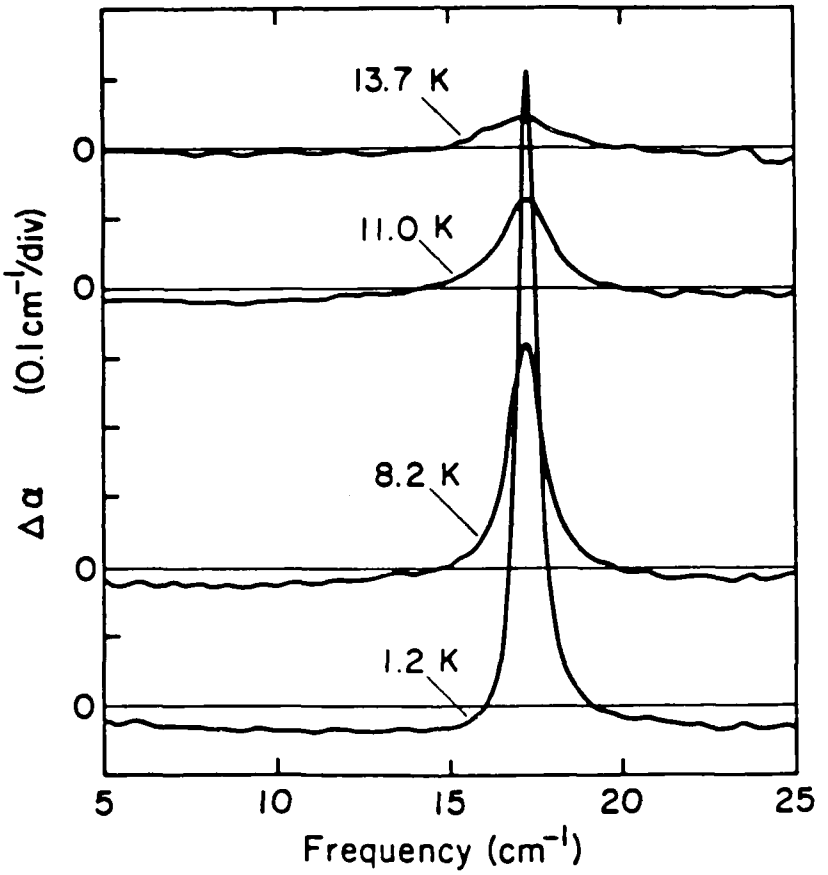

FIG. 1: Temperature induced change in the absorption coefficient for KI:Ag^+. $\Delta\alpha=\alpha(T)-\alpha(20.6K)$ and T for each trace is given in the Figure. Both the nonresonant and resonant mode absorption are evident in the bottom trace. The spectral resolution is 0.43 cm^{-1}.

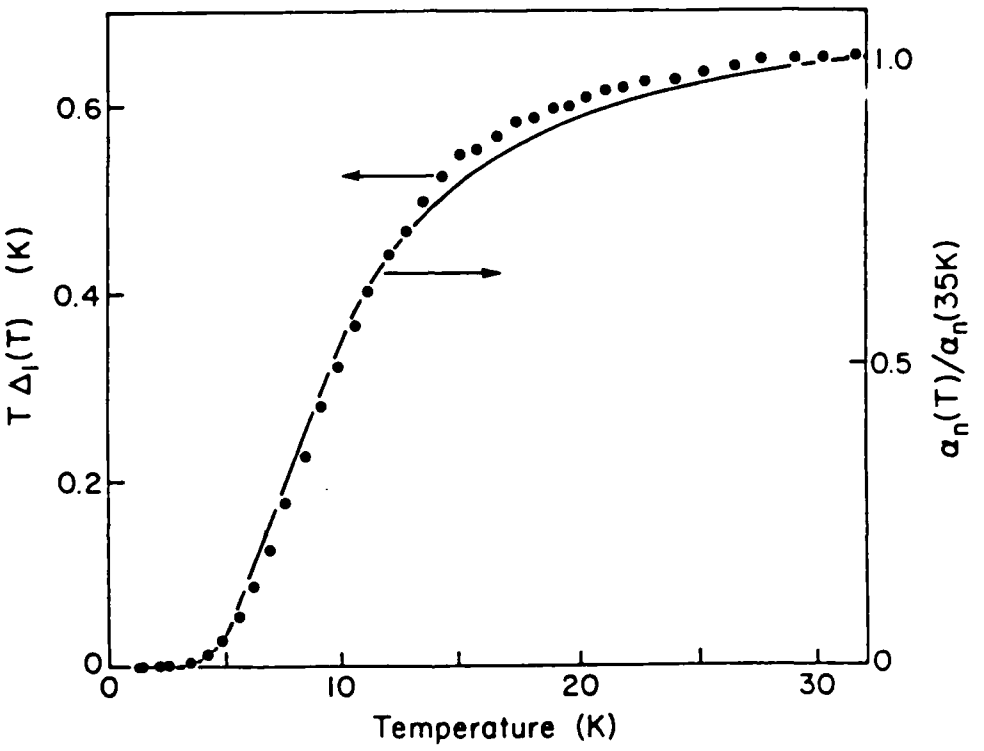

FIG. 2: (Solid curve, right ordinate) Normalized nonresonant far infrared absorption coefficient at 4 cm^{-1} vs temperature. The normalization factor is the high temperature value. (Dotted curve, left ordinate). Temperature dependence of $T\Delta_1$ which is proportional to the population in the second configuration for $KI:Ag^+$. The initial increase of the data with temperature follows an energy gap law with gap=24K.

and N is the impurity number density, p the dipole moment, k, Boltzmann's constant, T, temperature and τ the relaxation time. According to Eq. 1 for the far infrared limit ($\omega\tau \gg 1$), the absorption coefficient is

$$\alpha_n = \frac{\Delta_0}{c\sqrt{\varepsilon_0}} \left(\frac{1}{\tau}\right) \qquad (3)$$

which is independent of frequency. If the Debye model describes the non-resonant absorption data then besides the far infrared signature in the absorption coefficient there should also be a radio frequency signature in the real part of the impurity induced dielectric function. We have looked for this effect.

Our measurements[4] at 10 kHz of the temperature dependent dielectric properties of KI:Ag^+ are shown in Figure 3. Although $\varepsilon_1(T)-\varepsilon_1(1.4K)$ shows a maximum at about 10°K, no corresponding loss peak is observed in $\varepsilon_2(T)$ as expected; moreover, the spectra shown in Figure 3 are independent of the excitation frequency. Both of these results indicate that $\omega\tau \ll 1$ over the entire temperature range of our measurements. Equations 1 and 2 show that in this limit $\Delta_1=\Delta_0 \propto N(T)/T$ so that the temperature dependent measurement of the real part of the dielectric constant provides a direct determination of the population.

To show the temperature dependence of the population in this second configuration, the data in Fig. 3 for 0.5 mole % AgI in KI are subtracted from pure KI, the result multiplied by T and plotted vs. temperature in Figure 2 (the ordinate on the left). At high temperature the data points indicate that the off-center population levels off at a constant value. Information about the reorientational relaxation time for Ag^+ in KI can be obtained by combining the experimental results for the dipole moment from the radio

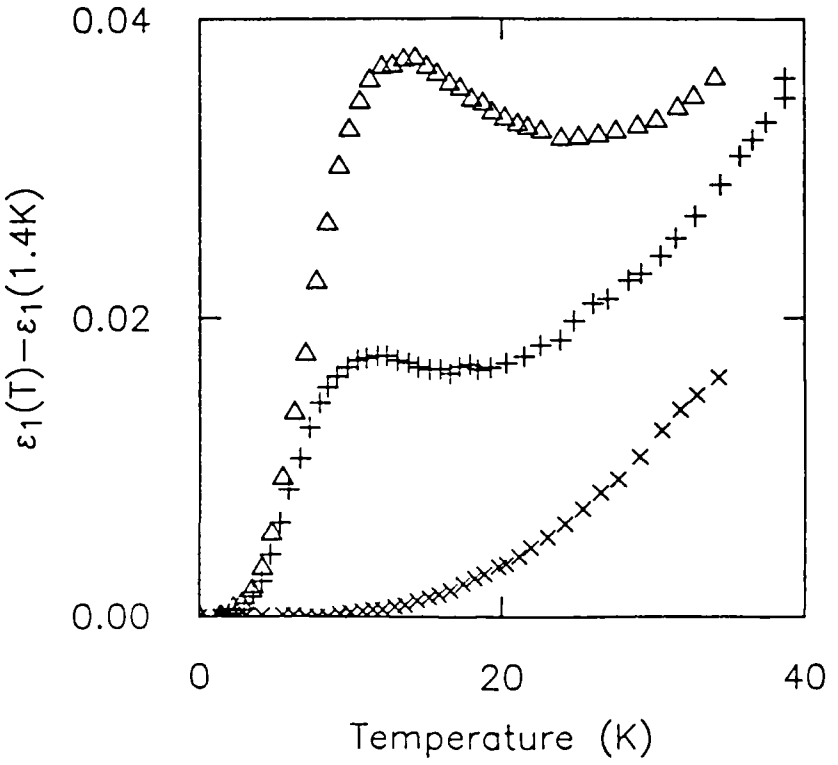

FIG. 3: Temperature dependence of the impurity induced dielectric constant for KI:Ag^+. $\varepsilon_1(T)-\varepsilon_1(1.4K)$ is plotted versus temperature for single crystal samples of 0.5 and 0.2 mole % AgI in KI (the triangles and crosses respectively). Also shown is the temperature dependence of $\varepsilon_0(T)-\varepsilon_0(1.4K)$ for pure KI (the x's). $\varepsilon_2(T)$ is temperature independent and the same value for all three samples (1.5×10^{-3}).

frequency dielectric constant measurement with the measured temperature dependence of the nonresonant absorption coefficient, α_n, in the far infrared spectral region. Inspection of Fig. 2 shows that the far infrared nonresonant absorption data follow N(T). Since Equation 3 predicts that the data should vary as $N(T)/[T\tau(T)]$, we conclude that $T\tau(T)$= constant.

The picture that emerges from our measurements is that two elastic configurations exist for this lattice-defect system. At low temperature the Ag^+ ion in KI is on center and resonant mode absorption is observed in the far infrared. When the temperature is increased a second elastic configuration which has an energy about 24°K above the ground state becomes populated. The large increase in the defect contribution to the dielectric constant indicates that the Ag^+ ion is off center in this second elastic state. Because the off-center population appears to approach a constant value at elevated temperatures we conclude that only these two elastic configurations are close by in energy.

The implications from this series of experiments are far reaching. The observation that the elastic ground state and first excited state are nearby in energy for the defect-lattice system may indicate that a series of elastic states are possible. These low lying elastic states should influence the thermodynamic properties in characteristic ways. For example, the low temperature specific heat should be larger than that calculated for a simple off-center impurity-lattice system because the additional elastic states increase the total number of states available at low temperatures. The implication from our study is that current theoretical lattice dynamic calculations are incomplete in that they underestimate the number of degrees of freedom that are available to the lattice-defect system at low energy.

2.2.2 Long Crystal Transmission Measurements

By making far infrared transmission measurements on KBr doped with Li^+ and NaCl doped with Cu^+ single crystals with sample lengths an order of magnitude larger (16 cm) than previously used by earlier workers, we have been able to identify three new features of lattice defect modes.[5]

i) Excited state resonant mode transitions are observed at frequencies far removed from those expected for a harmonic oscillator. Because of the large density of phonon states at the overtone energies, the excited state transitions in each lattice defect system are heavily damped with a characteristic Frohlich resonance shape. For KBr:Li^+ the observed overtone shift is not consistent with that produced by a small central barrier in an otherwise harmonic potential. The shift can be accounted for with a large quartic term in the potential but such an anharmonic contribution produces a large resonant mode Stark effect whereas only a small effect has been observed. Thus the available data for KBr:Li^+ do not appear to be consistent with potential models which have been used in the past. The observed overtone shift for NaCl:Cu^+ is consistent with a model which contains a Fermi resonance between two nearly degenerate E_g resonant modes; however, this model is not consistent with the KBr:Li^+ data. Why similar excited state spectra should require different explanations is a troublesome point which raises fundamental questions about all of the dynamical models which have been used to describe resonant mode systems. It may be that the inconsistencies which we have identified are simply ramifications of the two configuration model--a model which appears to describe the KI:Ag^+ data. In order to determine whether or not this is the case more accurate temperature dependent measurements with far infrared and Raman spectroscopic techniques are required on all of these lattice defect systems.

ii) Paraelectric modes in KBr:Li^+ occurring far below the resonant mode frequency have been identified with Li pairs. By monitoring the paraelectric mode strength with respect to the resonant mode excited state strength for a given temperature interval it has been possible to show that the paraelectric mode strength varies nearly quadratically with Li^+ concentration. The (50-50) Li^+ isotope mixture in KBr experiment confirms the pair mode assignment. If pair modes are important then in such a crystal 25% of the centers will be $^6Li^+$ pairs, 25%, $^7Li^+$ pairs and the remaining 50%, $^6Li^+$-$^7Li^+$ pairs.

The combination modes are easily seen in Fig. 4 where high resolution spectra below 10 cm^{-1} are shown for KBr with different isotopic mextures of Li^+ dopant. The concentrations of $^6Li^+$ (curve a) and $^7Li^+$ (curve c) are measured spectroscopically to be about the same ~3 x 10^{18} cm^{-3}. If the absorption lines in trace (b) of Figure 4 were associated with isolated Li^+ ions then the resultant would be a simple sum of curve (a) and curve (c); however, if the modes are due to dynamically coupled Li^+ pairs, then new modes should appear when the two isotopes are mixed. Inspection of Figure 4 demonstrates that the isolated ion model cannot account for curve (b). The three highest frequency modes are clearly identifiable with pairs because the new strong line in curve (b) at 5.5 cm^{-1} does appear to be about twice as strong as the 6.35 cm^{-1} ($^6Li^+$-$^6Li^+$) and the 4.8 cm^{-1} ($^7Li^+$-$^7Li^+$) lines. Moreover, the frequency of this new combination mode is halfway between the frequencies of the other two modes. The actual absorption strengths of these three modes are uncertain because of band overlap. Within these uncertainties the $^6Li^+$-$^6Li^+$ and $^7Li^+$-$^7Li^+$ induced absorptions are of equal strength and each half as strong as the $^6Li^+$-$^7Li^+$ induced absorption.

The intriguing experimental finding is that isolated Li^+ ions do not tunnel but Li pairs do. Whether this lattice defect corresponds to a Li_2^+ molecular ion

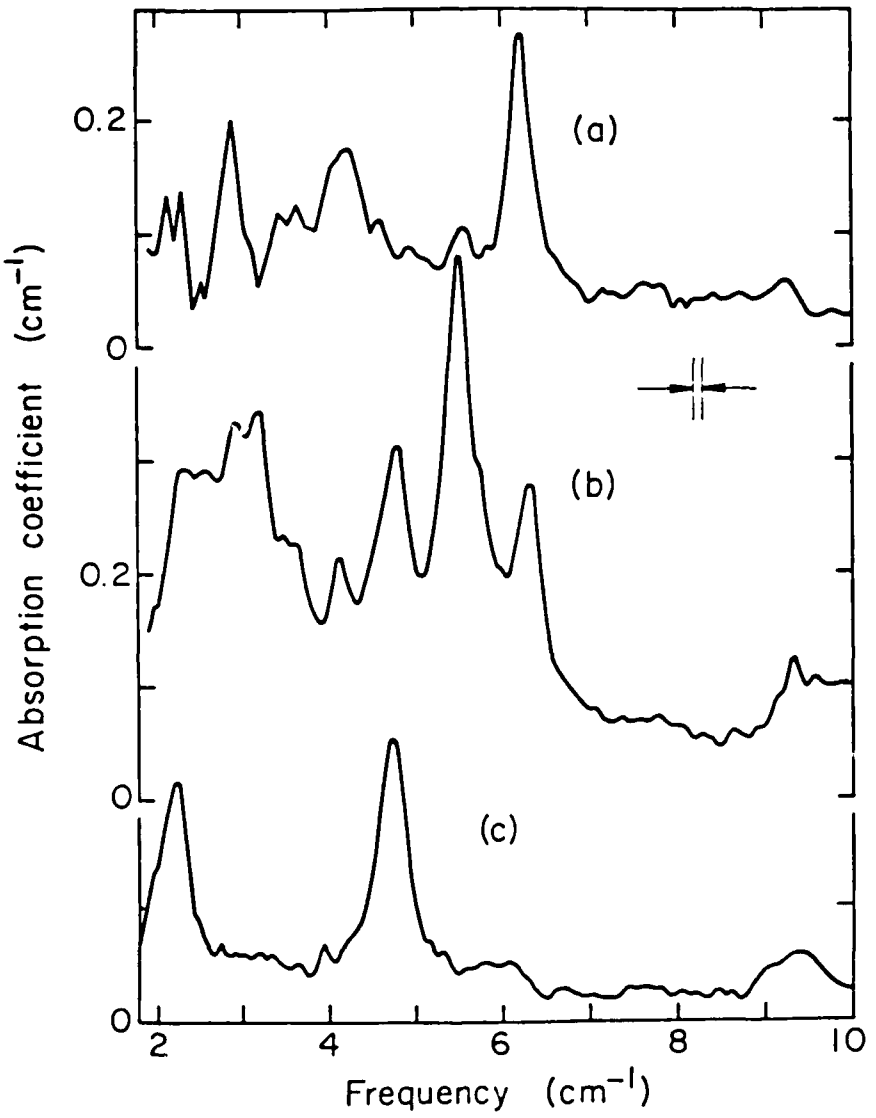

FIGURE 4: Impurity induced absorption spectra from 2 to 10 cm^{-1} for different isotopic mixtures of Li doped KBr. The sample temperature is 1.2 K and the instrumental resolution is 0.1 cm^{-1}. The dopand concentrations are as follows:
(a) 3 x 10^{18} cm^{-3} ^{6}LiBr,
(b) 3.8 x 10^{18} cm^{-3} ^{6}LiBr + 3.8 x 10^{18} cm^{-3} ^{7}LiBr,
(c) 3 x 10^{18} cm^{-3} ^{7}LiBr. Note that new modes appear in the combination crystal spectrum (b) which are not seen in (a) or (c).

or to two next nearest neighbor Li^+ ions has not been resolved.

iii) Another unusual feature of the KBr:Li^+ spectrum is that weak satellite modes with transitions near the resonant mode frequency do not stem from pairs but are associated with isolated Li^+ impurities. These modes could be associated with Li complexes or Li^+ in another lattice site, e.g. an interstitial, but it is unlikely that either a complex or a different site would produce a resonant mode with nearly the same frequency as for the substitutional impurity. The $^6LiOH^-$ molecule in KBr showed no strong absorption lines in this spectral region.

In long crystals of NaCl:CuCl a pair spectrum was identified at frequencies below the resonant mode transition but no high frequency satellites were observed. The absence of a measurable isotope splitting in this spectrum indicates that the pair modes probably are not associated with tunneling motion.

2.3 Molecular Vibrations In Crystals

2.3.1 Discovery of persistent pegs

Four years ago we discovered that persistsent holes could be burned into the vibrational mode spectrum of ReO_4^- molecules in alkali halide lattices.[6] After a variety of low temperature laser experiments it became clear that the effect we were studying was very similar in behavior to persistent spectral nonphotochemical hole burning (NPHB) which had been reported for a number of inhomogeneously broadened optical transitions in glasses.[7] The difference was that persistent spectral holes observed for electronic transitions were thought to arise because of two level systems in the matrices. Our observation that persistent spectral holes could be burned in the vibrational absorption spectrum of a high-symmetry photostable molecule in a simple, ordered crystalline host demonstrated that the effect was more general than previously expected.

The model that evolved out of our early study was very similar to that used by Hayes, Stout and Small to explain NPHB in glasses.[7] The principal difference was that for our compound the configurational degeneracy is provided by the optically active site itself rather than by the presence of the nearby tunneling systems in the host matrix.

Although this model predicts the correct experimental behavior a fundamental problem has been that it also predicts librational states in the broad band absorption spectrum yet none are observed.[8] This mystery has been resolved with the discovery of the antihole or peg.[9]

Figure 5 shows a transmission spectrum of a thick alloy sample (KI+0.05% $KReO_4$+2%NaI) at 6K as measured with a high resolution fourier transform spectrometer. The doublet structure of the ν_3 mode comes from the two Re isotopes. The two doublets farthest removed from the unperturbed mode at 923.5 cm^{-1} appear because of a nearby Na^+ impurity. The close in doublets come from Na^+ impurities further away from the ReO_4^- ion. The laser coincidences for both N_2O and CO_2 lasers for all perturbed ν_3 frequencies are also indicated in Fig. 5. The important experimental observation is that now a number of gas laser transitions are coincident with vibrational modes.

The persistent holes which can now be hurned using N_2O, P19 are very similar in behavior to those found earlier by burning with CO_2, P42 in the main ν_3 band. band. The surprising result is that at N_2O, P17 a persistent antihole (peg) is produced.

An enlargement of the important spectral region is shown in Fig. 6A. A spectroscopic measurement of the peg has been made with a tunable low power diode laser. A first derivative spectrum of the peg is shown in Fig. 6B. The line shape corresponds to a central line of enhanced absorption with a full width at

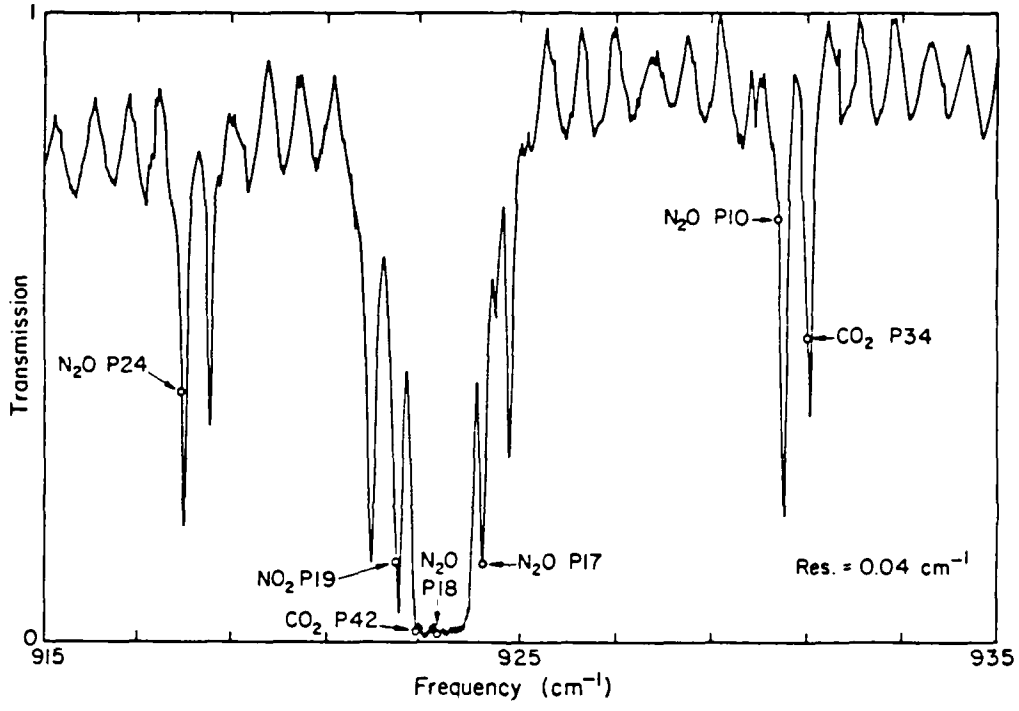

FIGURE 5: High resolution spectrum of KI + 0.05% $KReO_4$ + 2% NaI showing laser coincidences at T=6K.

half maximum of 28 MHz, but surrounded by broad wings of decreased absorption. The overall shape is a negative replica of the persistent hole which had been observed at 10 P42. A reexamination of other ReO_4^--host lattice combinations at a number of N_2O frequencies has shown that this peg formation is quite general. Persistent holes or persistent pegs occur depending upon the particular spectral position at which irradiation occurs.

The idea that narrow-band laser radiation within an inhomogeneously broadened absorption line might lead to a burned spectral hole through saturation, photodecomposition, photoinduced reorientation or perhaps other processes which remove absorbers from the spectral region under irradiation is no longer very surprising. An increased absorption at the frequency of irradiation is not so easy to explain.

A simple but subtle variation in the model used earlier appears to account qualitatively for the persistent hole and peg phenomena. We imagine that the local lattice strain gradients make the two ground state arrangements, A and B, of the tetrahedral molecule in the cubic site inequivalent. In addition it is assumed that the two configurations in the excited vibrational states A' and B' are different from the ground state as shown in Fig. 7. Although the random nature of the strain field produces distributions of all of these energy levels, the important features with respect to hole and peg production can be demonstrated with the four levels shown in Fig. 7. In arrangement (1) the potential-well asymmetry in the ground state is larger than the asymmetry in the excited state while the converse is true for arrangement (2). For both cases well asymmetry is assumed to be large compared to the tunnel splitting so the infrared selec-tion rule strongly favors left well-left well or right well-right well transitions.

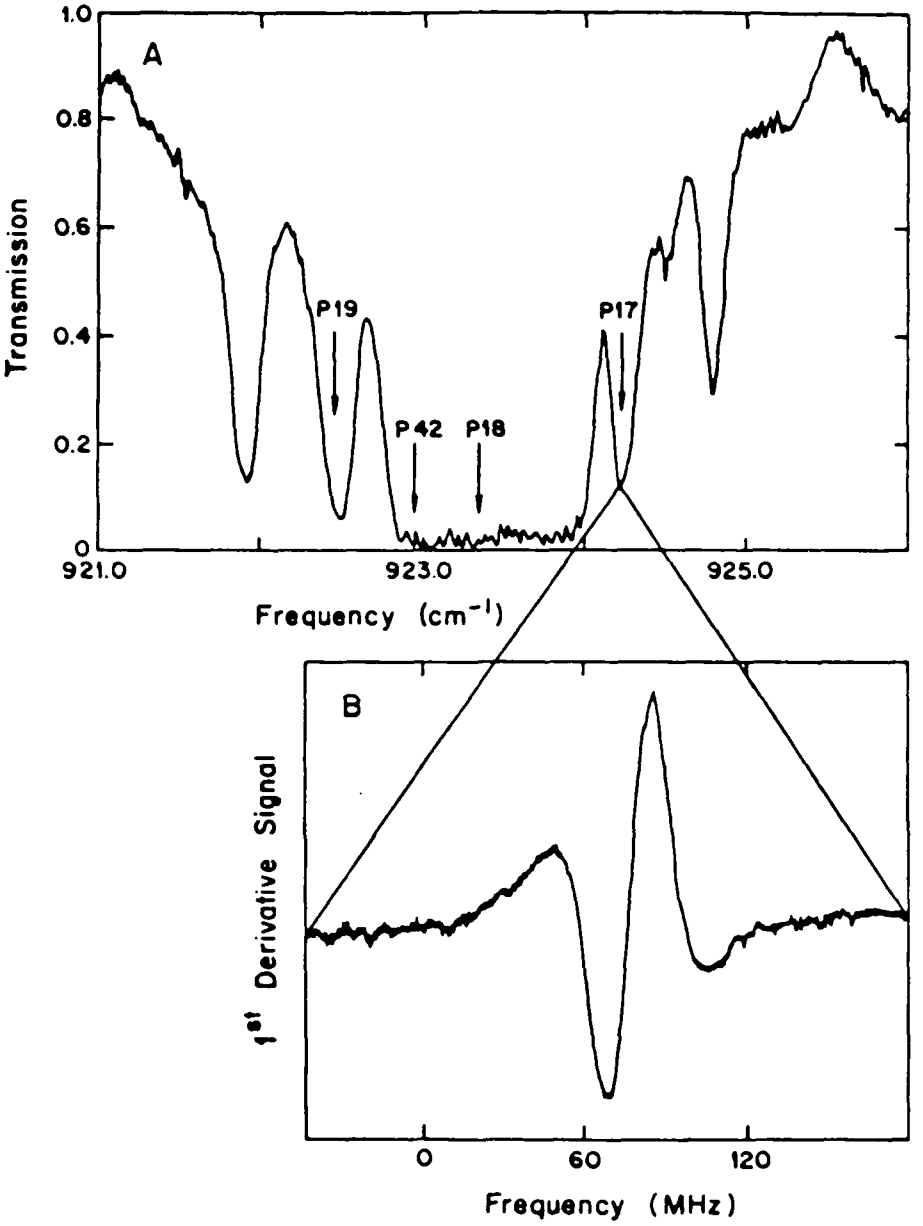

FIGURE 6: (a) Infrared transmission spectrum of KI + 0.05% $KReO_4$ + 2% NaI in the region of the ν_3 mode. (b) diode laser first derivative spectrum of the peg at N_2O P17. The central feature corresponds to enhanced absorption.

These transitions are labeled AA' and BB' in the lower part of the Figure. The nearly forbidden transitions between configurations, labeled AB' and BA', are the pathways that lead to persistent elastic polarization of the resonant molecules.

When the laser frequency ω_p is not symmetrically located with respect to the AA' and BB' transition frequencies in Fig. 7 persistent spectral effects are produced. For the energy level arrangement (1) the laser pump drives centers from A to B via the overlap of the laser with the homogeneous width of the AB' transition. Since the number in A decreases, the strength of AA' decreases and a hole appears at the pump frequency. For the energy level arrangement (2) the laser pump again drives centers from A and B via the AB' transition but increased absorption now occurs near ω_p since the dominant absorption results from the overlap of the homogeneous width of the BB' transition with the laser line instead of the AA' transition.

2.3.2 Ultrasonic studies of persistent holes and pegs

The model represented by Fig. 7 requires that the tetrahedral molecular ion has two rotationally equivalent configurations at the substitutional lattice site which are separated by a large energy barrier due to steric effects and which, infact, have slightly different energies due to local strain gradients in the crystal.

A measurement of the temperature dependent absorption of 10 MHz ultrasound in RbBr, KI and RbI crystals doped with ReO_4^- has produced the first direct experimental identification of a two configuration energy barrier associated with this defect-lattice system.[10] The loss peak stems from an activation process with a barrier height of 60 meV for RbBr, 50 meV for KI and 30 meV for RbI. The decreasing barrier height with increasing lattice constant may account for the

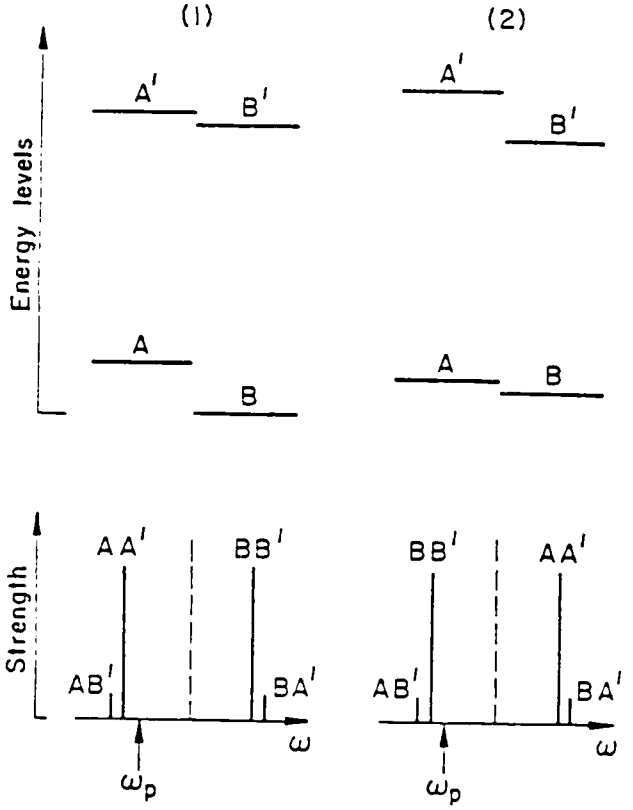

FIGURE 7: Photoinduced reorientation model for ReO_4 in alkali halides. Two possible configurations denoted A(A') and B(B') occur for each zero libration state. Arrangement (1) has the double-well asymmetry of the two ground-state configurations larger than for the two excited states and arrangement (2) has the opposite. The bottom figure shows the line strengths vs frequency for each of the transitions in the two arrangements.

observation that spectral holes are burned and erased most easily in the RbI host.

The combination of ultrasound with the persistent spectroscopic effects has led to the development of a new phase-insensitive optical detector for ultrasonic waves in solids.[11] When ultrasonic waves are applied to an alkali halide which contains persistent holes or pegs the hole depth or peg height is modulated. This effect occurs because the local ultrasonic strain introduces a variety of frequency shifts which add up to a broadening of the persistent feature. Since, at the hole's [peg's] center frequency, the absorption can only increase [decrease] due to these frequency shifts; the transmitted signal reflects the rectified displacement. Such a process is completely independent of the phase of the ultrasound, provided that the acoustic wavelength is smaller than the beam diameter.

An estimate of the sensitivity of this new optical method of ultrasonic detection has shown that for the ReO_4^- molecule an ultrasonic wave amplitude of 1Å should be easily detectable. Even more sensitivity can be obtained by using the persistent photochemical hole of the F_3^+ center in NaF where it was predicted that for 10 MHz sound an amplitude of 10^{-2}Å could be detected.[11] A recent study of this defect-lattice system has confirmed and extended these ideas.[12]

2.3.3 Observation of an unbleachable ν_4 mode in $BH_2D_2^-$

The systematic investigation of the transient and perisitent hole burning properties of the ν_3 mode in ReO_4^- molecules in alkali halide crystals has produced a detailed understanding of the microscopic mechanisms responsible for the decay of the excited vibrational state. The results showed that at low temperatures the decay channel consists of multistep emission of other internal modes, localized phonon modes and band phonons. It has been the intrinsic symmetry and symplicity of this hole burning system which has enabled us to study many aspects of the anharmonic decay process. One key result has been that the ν_3 mode can decay into the low lying ν_4 mode of this spherical top molecule which is near in energy to the phonon spectrum.

The work described in this section was motivated by the desire to study the vibrational relaxation of spherical top molecules in which the lowest frequency mode, the ν_4, was situated in the 10 μm wavelength region coincident with our CO_2 laser.[13] Our initial effort was with ND_4^+ a spherical top which can be diffused into alkali halides. The variation of the ν_4 mode frequency with lattice constant is shown in Fig. 8. Although the mode occurs in the R branch region of the CO_2 laser, a low temperature coincidence has not been observed because of temperature dependent mode narrowing.

The next study focused on BH_4^- which again can be doped into alkali halide crystals by diffusion and has a mode near the top end of the CO_2 R branch. With the sample cooled to liquid helium temperature we found that the ν_4 mode of BH_4^- is above the CO_2^- P branch range. The solution to this coincidence problem has been to diffuse both BH_4^- and BD_4^- molecules at the same time. Because of isotope exchange molecules of BH^3D^-, BH^2D^2 - and BHD^3 -

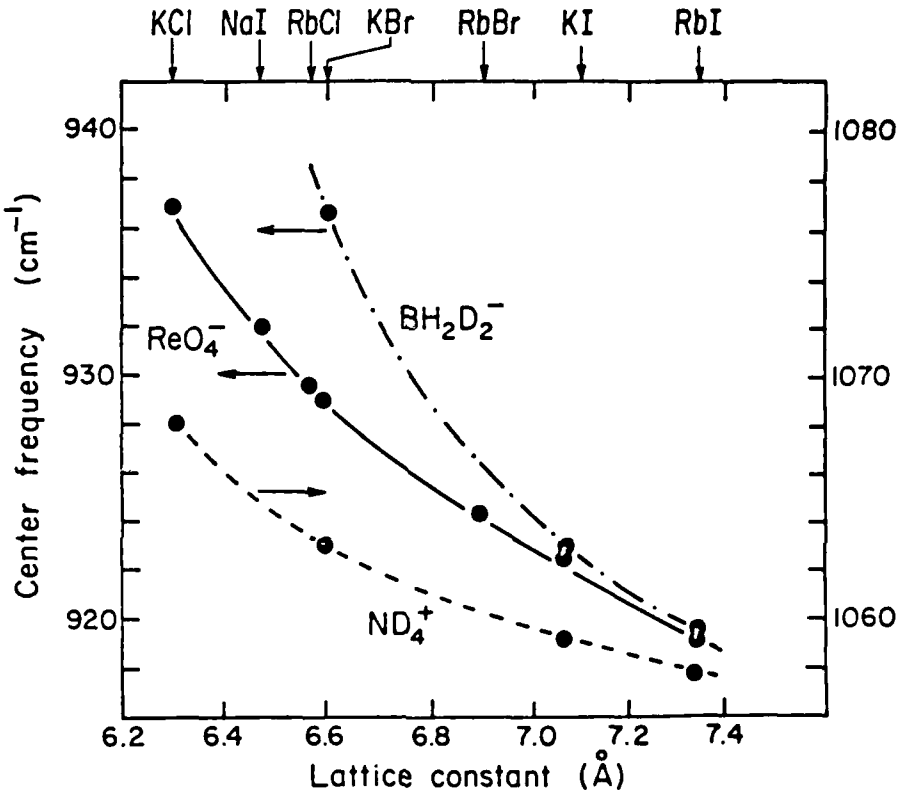

FIG. 8 Vibrational mode frequency versus host lattice constant. The spherical top molecules are identified in the figure. The data were obtained with room temperature samples.

appear in the crystal and the low frequency modes of these molecules are in the CO_2 laser tuning range.

The lowest energy internal vibrational mode of $BH_2D_2^-$ in KBr at low temperatures is coincident with a strong CO_2 laser line, 10P22 (942 cm^{-1}). The frequency dependence of this mode with host lattice is shown in Fig 8. Note that the mode tunes more rapidly with host lattice than does the ν_3 mode of ReO_4^-.

A transmission spectrum in the 10 μm region of a KBr crystal doped with the 5 isotopically different spherical top molecules is shown in Fig. 9. The letters labeling the various absorption lines refer to the vibrational mode assignments. The assignments were made by calculating the mixed isotope mode frequency positions using the pure isotope mode frequencies as input parameters. Of interest here is the line labelled B which corresponds to an intermediate frequency nondegenerate vibration of $BH_2D_2^-$.

A comparision of the vibrational energy level diagrams for ReO_4^- and $BH_2D_2^-$ is shown in Fig. 10. The lower case letters indicate the three non degenerate ν_4 modes of $BH_2D_2^-$, while the ν_3 and ν_4 modes of ReO_4^- are three fold degenerate. The arrow indicates the transition pumped in each system by the high power CO_2 laser. If multiphonon relaxation is important for both molecules then the larger energy gap for the ν_4 mode of $BH_2D_2^-$ compared to ReO_4^- would suggest that $\tau(BH_2D_2^-) >> \tau(ReO_4^-)$. Experimentally we have found the opposite to be the case!

No bleaching of the $BH_2D_2^-$ vibrational mode was observed even with CO_2 intensities of $1MW/cm^2$ and the sample cooled to 1.7K. From this result and a measurement of the low temperature inhomogeneous width (which must be larger than the homogeneous width) a conservative upper limit to the relaxation time

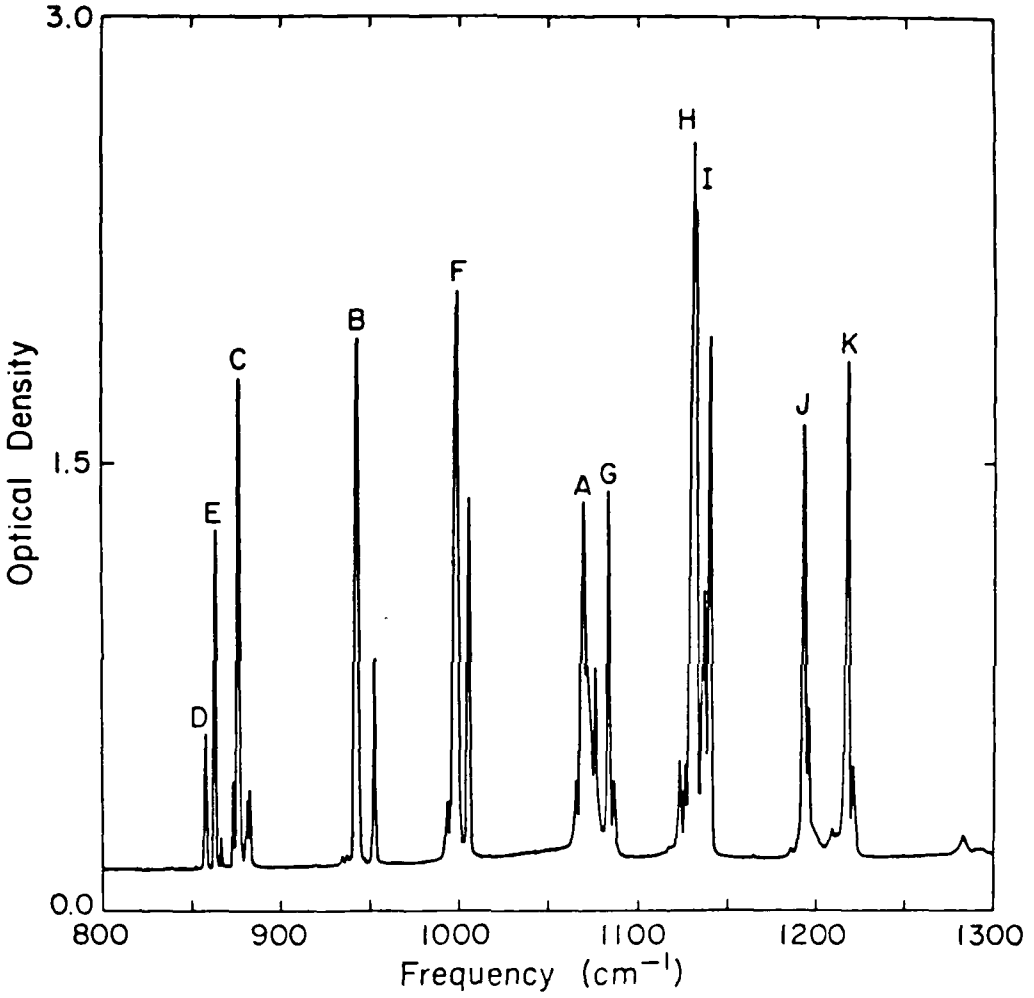

FIG. 9 Low temperature spectrum of a KBr crystal doped with BH_4^-, BH_3D^-, $BH_2D_2^-$, BHD_3^- and BD_4^-.

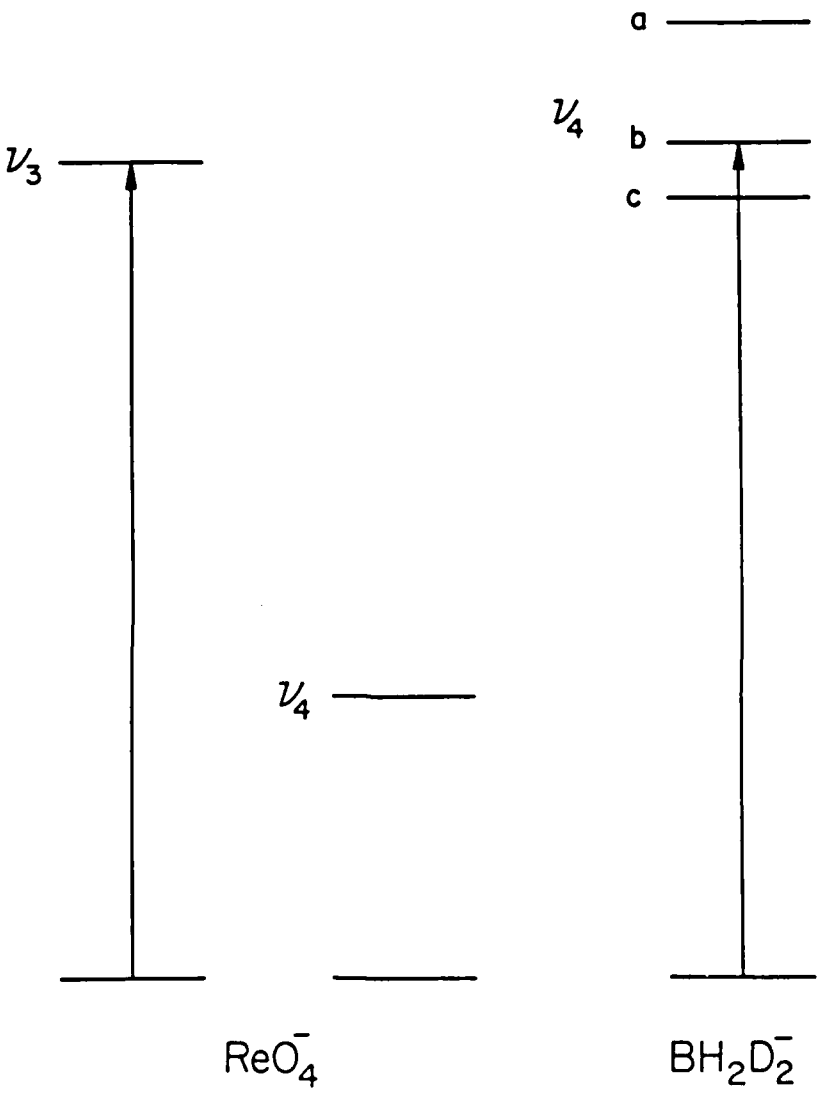

FIG. 10 Vibrational energy level diagram of ReO_4^- and $BH_2D_2^-$ at low frequencies. The three fold degenerates ν_4^- mode of ReO_4^- which is important in the anbarmonic decay of the three fold degenerate ν_3^- mode is indicated. The $BH_2D_2^-$ modes are nondegenerate. The arrows identify the pump laser frequency used in the saturation experiment.

can be obtained. We find that $\tau(BH_2D_2^-)<20$ psec whereas $\tau(ReO_4^-)=4.5$ nsec. Just why the relaxation of the ν_4 mode of $BH_2D_2^-$ is so fast is not yet clear.

One difference between ReO_4^- and $BH_2D_2^-$ is that the former has a very large mass (250 amu) while the latter is very small (15 amu). Although the ν_4 mode of $BH_2D_2^-$ is far removed from the normal phonon spectrum the small mass defect would be expected to produce a local mode with frequency above the normal band mode region. If the ν_4 decay mode made use of this high frequency external mode then the decay would occur in lower order and hence be faster. Such a local mode has been observed[14] for BH_4^- in RbI. Extrapolating from this work using the lattice constant dependence of the U center local mode in alkali halides we find that the local mode frequency of $BH_2D_2^-$ should occur at about 210 cm^{-1}. If this feature is the important decay channel then a four local mode plus one band mode process is required to relax the excited vibrational state. This is the same order of multiphonon decay that was required to explain the ReO_4^- data so the two relaxation times should be about the same. The experimental result is that the ν_4 mode of $BH_2D_2^-$ relaxes at least three orders of magnitude faster than does the ReO_4^- vibration.

Another possible explanation for this anomaly that we tracked down had to do with the known Fermi resonance[14] between $2\nu_4$ and ν_3. Because of the strong coupling between these two vibrational ladders perhaps the CO_2 laser pumping simply populated both ladders so that saturation would no longer be possible and the analysis used in the previous paragraphs would be incorrect. A search of the infrared and visible showed that no vibrational or electronic fluorescence occurs for this defect.

Our tentative explanation of the absence of high power bleaching of the ν_4 mode in $BH_2D_2^-$ is that both the local mode and the Fermi resonance mechanism are required. The local mode insures that the decay process is as fast as ReO_4^- (τ~5nsec) and the Fermi resonance assures that a large reservoir of levels is available so that bleaching cannot occur. Since the vibrational fluorescence radiation time is ~1msec, it is completely quenched by multiphonon relaxation. The end result is that $BH_2D_2^-$ is a nonsaturating molecule. We now use these particularly sharp vibrational absorption lines for narrow band rejection filters in the CO_2 laser region.

2.3.4 KBr:CN^-:Na^+, a vibrational defect which hole burns and fluoresces in the IR

2.3.4.1 Introduction

By using a F.T. interferometer together with diode laser sources we have discovered a large number of vibrational modes associated with molecular defects in alkali halide crystals. In many cases the resolution of the F.T. interferometer is insufficient to resolve the inhomogeneous line widths of these modes. A particularly noteworthy example of this effect can be seen in alkali halide crystals doped with KCN. The resultant spectrum shows that both CN^- and NCO^- occur in the crystal. A high resoltion spectrum of 0.1 mole % KCN in KBr is shown in Figure 11. The spectral lines for frequencies larger than 2100 cm^{-1} stem from different isotopes of NCO^-. The inhomogeneous width of each isotopic mode is 0.05 cm^{-1} as measured with a diode laser and no hole burning is exhibited for this linear triatomic molecule.

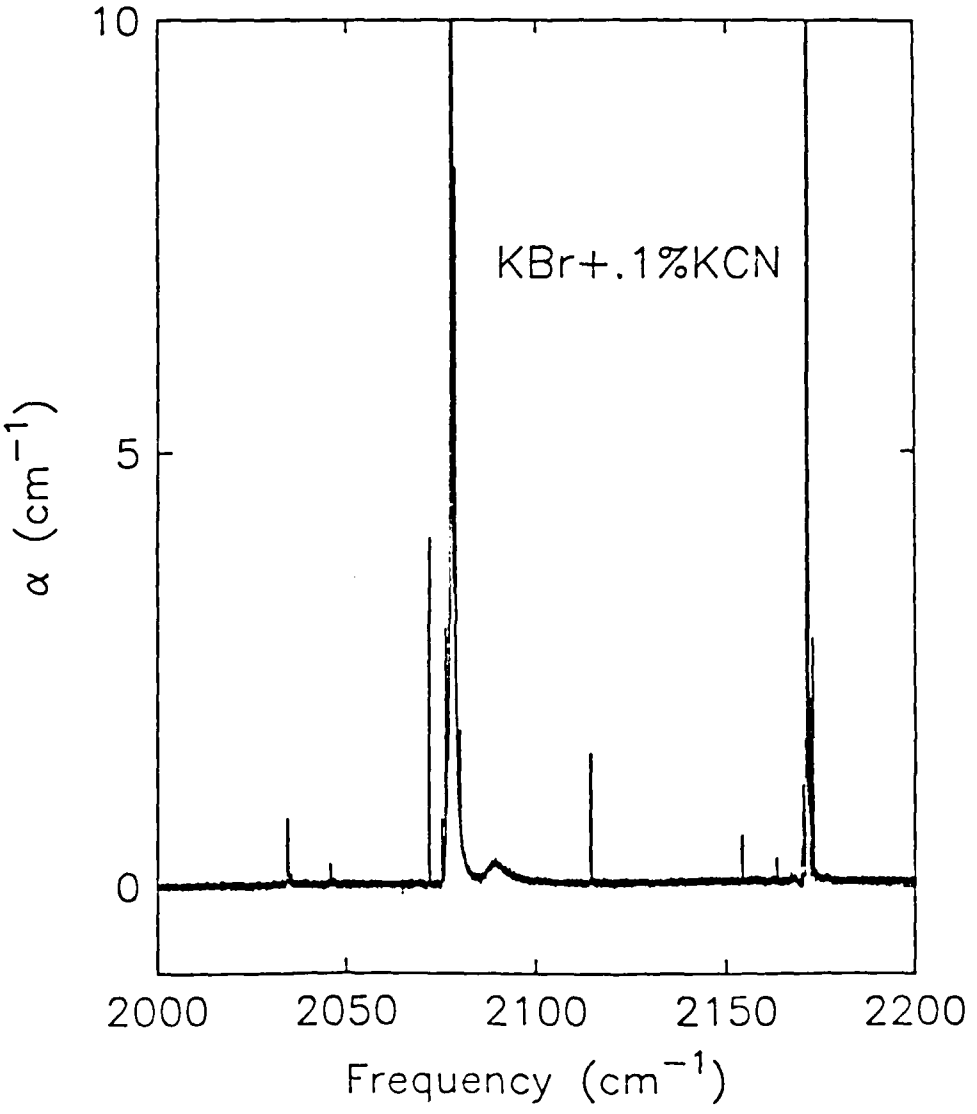

FIG. 11. Impurity induced absorption coefficient for CN^- doped KBr. The absorption lines at frequencies larger than 2100 cm^{-1} are associated with isotopes of NCO^- while the lines at lower frequences are associated with CN^-. Sample temperature is 1.7K.

The line spectrum shown in Fig. 11 for frequencies less than 2100 cm^{-1} is associated with the CN^- molecule. It is this spectral region where a number of new and unusual dynamical effects have been observed and in the rest of this section the features in this spectral region are described in some detail.

2.3.4.2 Permanent Hole Burning

Almost all of the sharp features show permanent hole burning when probed with a low power diode laser, but this hole burning is very different from that observed for the ReO_4^- molecule.[15] A typical spectrum for one of the vibrational modes centered at 2071.8 cm^{-1} is shown in Fig. 12. Note that the resolution of the probe is large enough that the absissa is now measured in GHZ. To burn sharp holes the diode power must be reduced to about 1 microwatt per cm^2 otherwise power broadening is observed.[16] After burning a hole for a few seconds the diode laser intensity is reduced still further and then the spectrum is scanned. The holes burned in this line are particularly long lived and show no change with time at liquid helium temperatures. In fact the holes are stable even if the sample is cycled up to 35K. To erase the holes the sample temperature must be increased to at least 50K.

What is the vibrational defect which produces such temperature stable holes? From a systematic investigation of the influence of second dopants on the CN^- vibrational spectrum, we have found that some of the sharp vibrational features are associated with perturbations produced by these other crystal impurities.[15] A spectrum of the impurity induced absorption for KBr + 0.2 mole % KCN + 0.2 mole % NaBr is shown in Fig. 13. Notice that the low frequency mode at 2071.8 cm^{-1} is much stronger than the same mode in

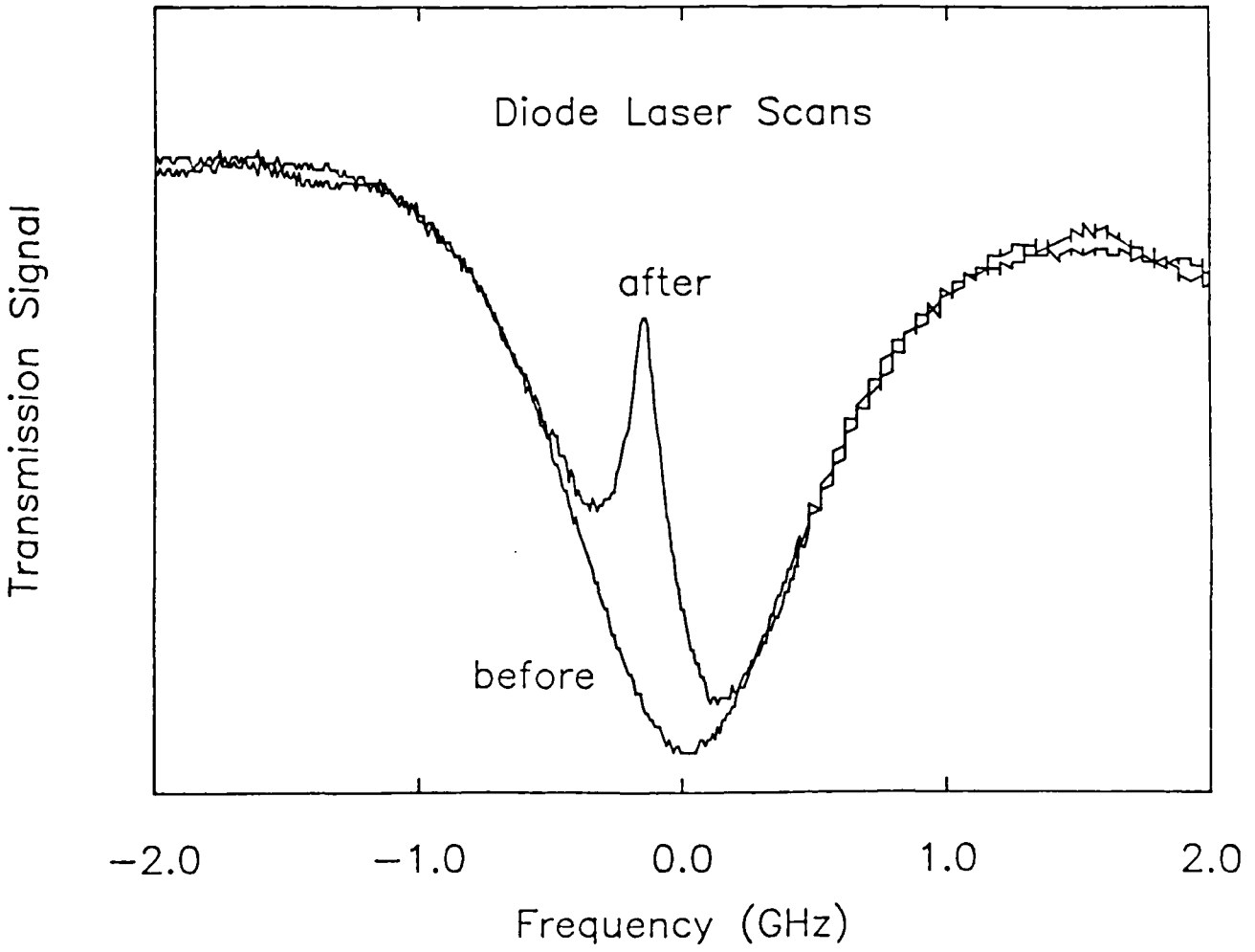

FIG. 12 Permant hole burning in the absorption line at 2071 8cm^{-1}. The spectral hole demonstrates that the absorption line is inhomogenerously broadened. Sample temperature is 1.7K.

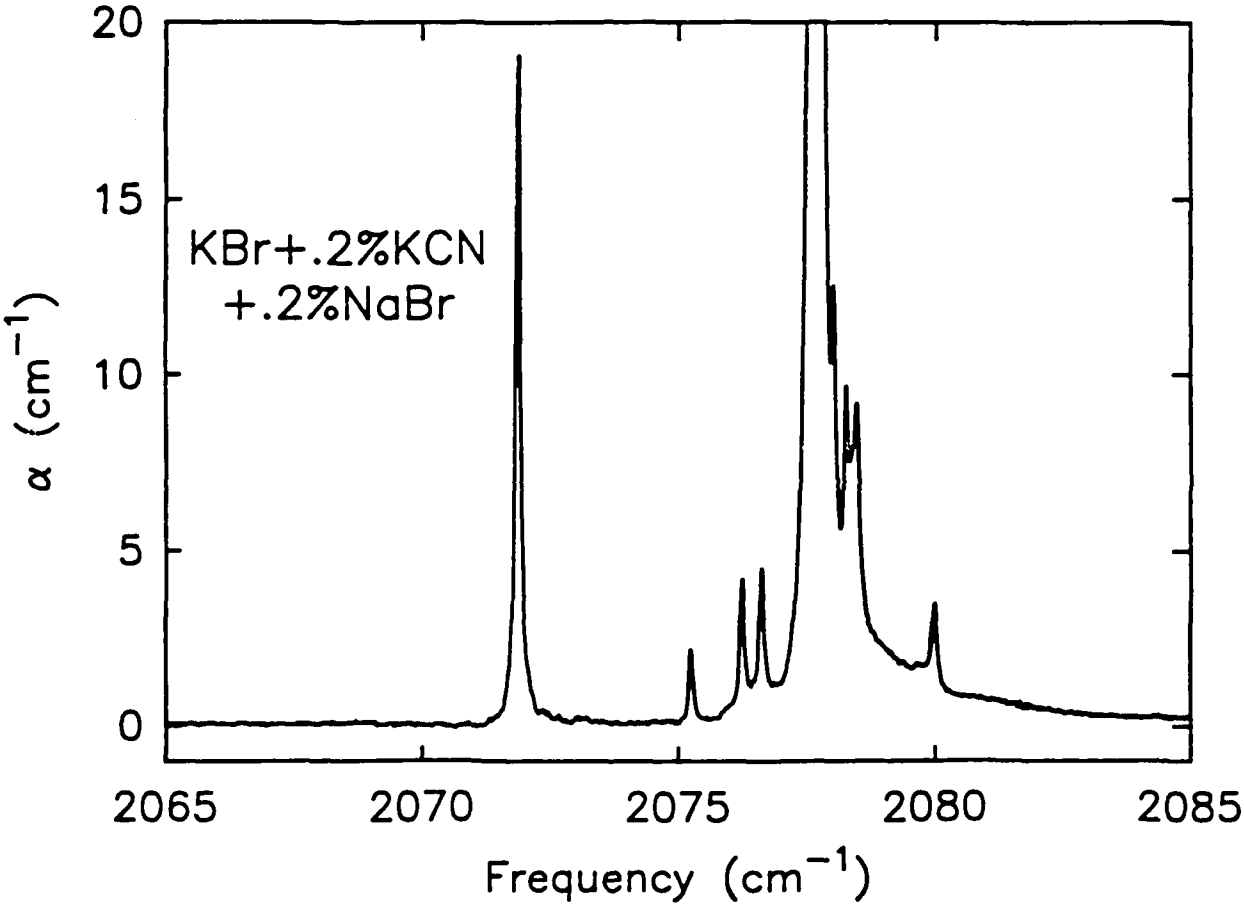

FIG. 13 Impurity induced absorption coefficient for CN^-:Na^+ doped KBr. The absorption line at 2071.8 cm^{-1} is proportional to the Na^+ concentration in the CN^- doped crystal. Sample temperature is 1.7K.

Fig. 11. Since this line has been observed to vary linearly in strength with the addition of NaBr to the melt, the vibrational mode is identified with a $CN^-:Na^+$ complex. Diode laser hole burning measurements have shown that this mode displays a number of interesting features. Polarization studies demonstrate that the center is oriented along the {100} axes of the crystal. Frequency dependent hole burning measurements show that the entire inhomogeneously broadened vibrational mode spectrum can be erased. By this I mean that if the diode laser is set on sweep mode at high power and swept over 2 GHz around the line center for a few minutes then when a low power scan is made of this frequency region the absorption line does not appear! For contrast it should be remembered that the ReO_4^- hole burning signature is completely different. If a hole is burned in the vibrational mode near a second hole then the second one fills in, i.e. the oscillator strength is only transferred over frequency intervals of a few 10's of MHz. The photophysical hole burning model described in Section (2.3.1) is consistent with this shift. For the $CN^-:Na^+$ defect, on the other hand, the oscillator strength is transferred to a completely different frequency region which is wavenumbers away from the diode operation point. Our development of a new spectroscopic technique which is described next has made possible the observation of the transfer of oscillator strength in the spectrum.

2.3.4.3 A New Method For High Resolution Spectroscopy in the Defect Solid State

The diode laser provides high resolution but has a limited tuning range while the F.T. interferometer has a large tuning range but limited resolution. This resolution is low enough that a hole burned with a diode laser cannot be resolved with the interferometer. Because the entire inhomogeneous CN-:Na+ line can be erased with the diode by running it in sweep mode, the

inhomogeneously broadened product state which will occur at a different frequency should be resolvable with the F.T. Interfermeter.

The experimental procedure with which this new state has been observed is as follows: First a F.T. spectrum of the CN^- spectral region is recorded with the sample maintained at 1.7K. Next the diode laser is swept with high intensity over the frequency region of the $CN^-:Na^+$ mode until the mode is erased. Finally a second scan with the F.T. spectrometer is made and the two absorption coefficients are subtracted from each other. The resultant spectra are shown in Fig. 14. The top trace shows the sample before the diode laser irradiation while the bottom trace shows the difference between the before and after spectra. Note that the diode laser has erased the line near 2072 cm^{-1} and a new feature appears near 2078 cm^{-1}. This new feature has exactly the same polarization as the absorption line which was erased. In addition this new line itself can be erased by application of the diode laser here and the oscillator strength returns to the low frequency position near 2072 cm^{-1}. The data indicate that the permanent hole burning and erasing effects at the two different frequencies occur because the C of CN^- is pointing at the Na^+ nearest neighbor in one arrangement while the N of the CN^- has this role in the second arrangement.[16]

2.3.4.4 Vibrational Mode Stark Effect

The first Stark effect measurements on a vibrational mode in the defect solid state[17] have shown that the dynamical rearrangement which occurs when the CN^- ion takes up its two inequivalent positions in the lattice is quite subtle. Figure 15 shows the absorption line at 2071.8 cm^{-1} with a persistent hole burned in the inhomogeneous line. The second trace shows the Stark

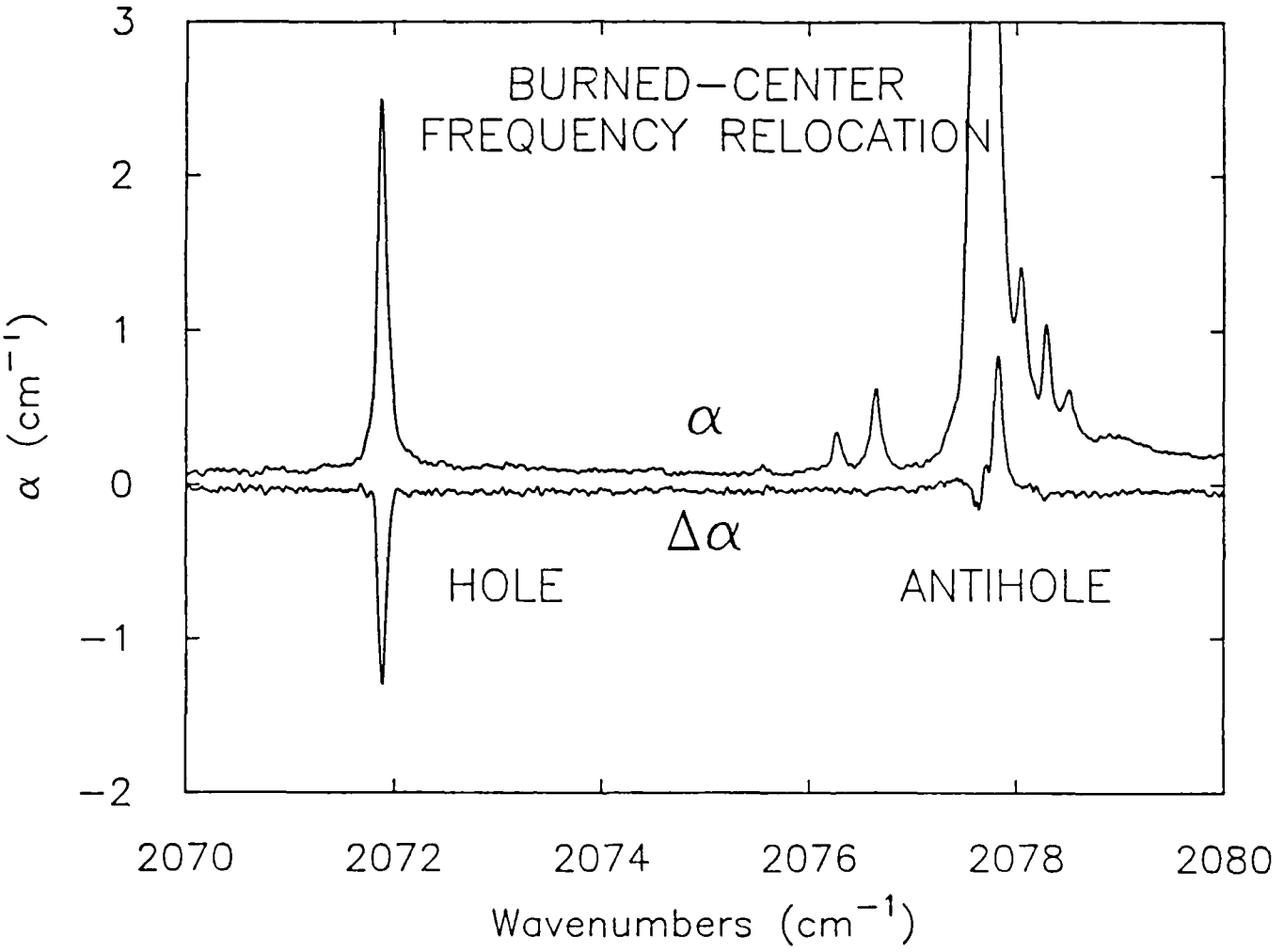

FIG. 14 Experimental demonstration of the relocation of vibrational mode oscillator strength for the $CN^-:Na^+$ line. The top trace shows the impurity induced spectrum before the 2071.8 line is erased with a diode laser. The bottom trace shows the difference between the two spectra (after-before). Sample temperature is 1.7K.

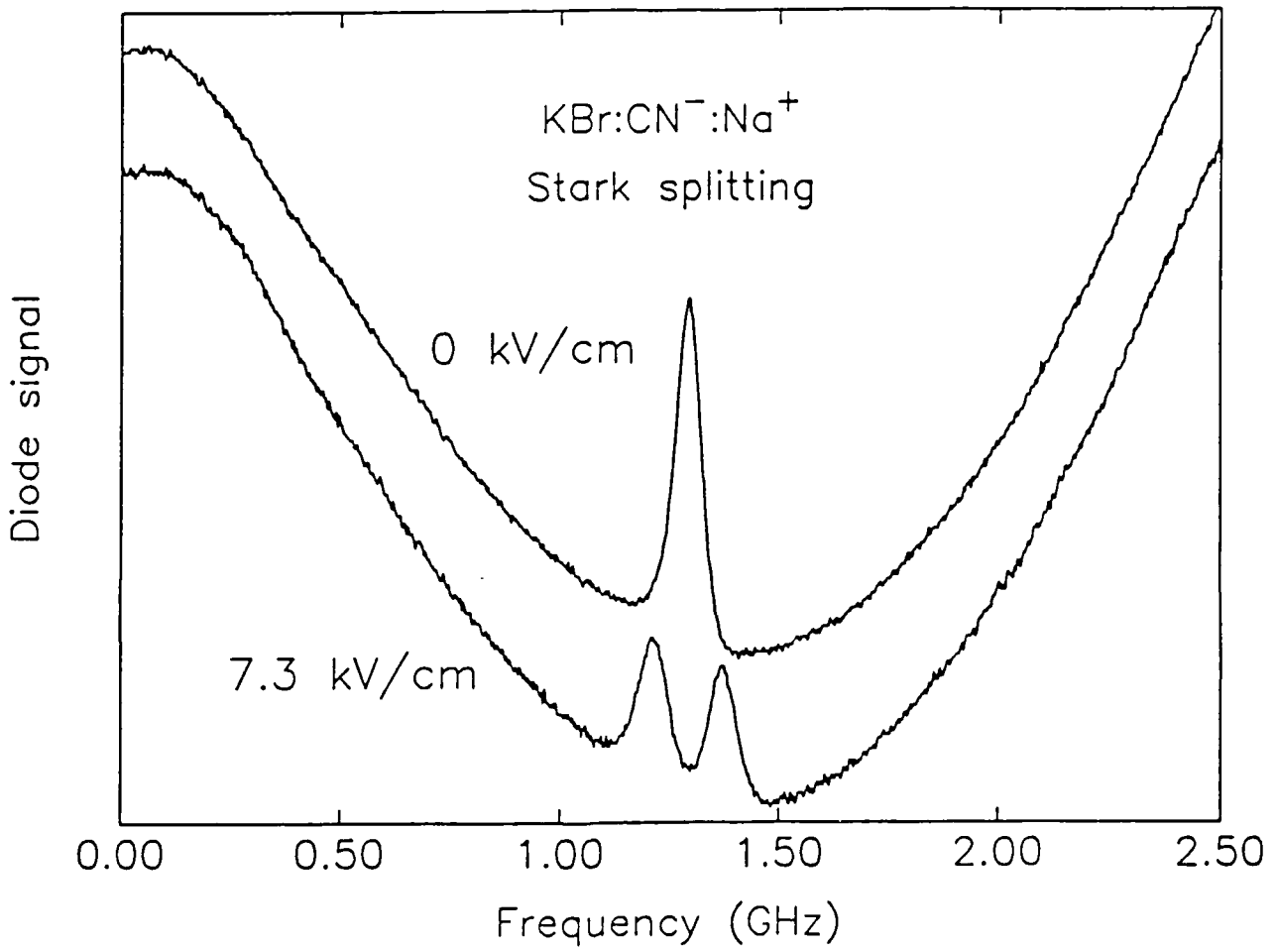

FIG. 15 Stark splitting of the permanent hole in the $CN^-:Na^+$ vibrational mode. Sample temperature is 1.7K.

splitting of this permanent hole which occurs when 7.3 kV/cm is applied across the sample. Since the splitting is linear in electric field, the effective dipole moment can be calculated. It is measured to be 0.02 Debye. The next step is to erase the entire line, producing a new line near 2078 cm^{-1} (as described earlier). A hole can now be burned in this line and the electric field applied to the sample. In this case we were surprised to discover that no Stark splitting is observed. Apparently there is enough rearrangement in the lattice that the effective dipole moment for one orientation is much smaller than for the other one.

2.3.4.5 IR Fluorescence of the $CN^-:Na^+$ Center

Another surprise has been our observation that the CN^-Na^+ center shows vibrational fluorescence[15] at 2071.8 cm^{-1}. The fluorescence was discovered while we were pumping the vibrational mode of isolated CN^- molecules with the second harmonic of CO_2 laser radiation at 2078 cm^{-1}. The flourescence spectrum as a function of frequency is shown in Fig. 16. Note that no fluorescence is seen at the pump frequency but many transitions appear to the low frequency side of the pump. Some of the transitions are identified in the Figure. Because of the V-V transfer between the isolated molecules the energy is transferred from site to site by resonant exchange until the excitation approaches a $CN^-:Na^+$ molecule. This molecule can be excited if the excited CN^- molecule emits a phonon. Once the excitation is in the $CN^-:Na^+$ vibrational state there are no phonons in the crystal to make up the energy difference between this vibrational state and the isolated CN^- so the vibration is therefore trapped until the $CN^-:Na^+$ center fluoresces. Therefore even though the concentration of these centers is very small they

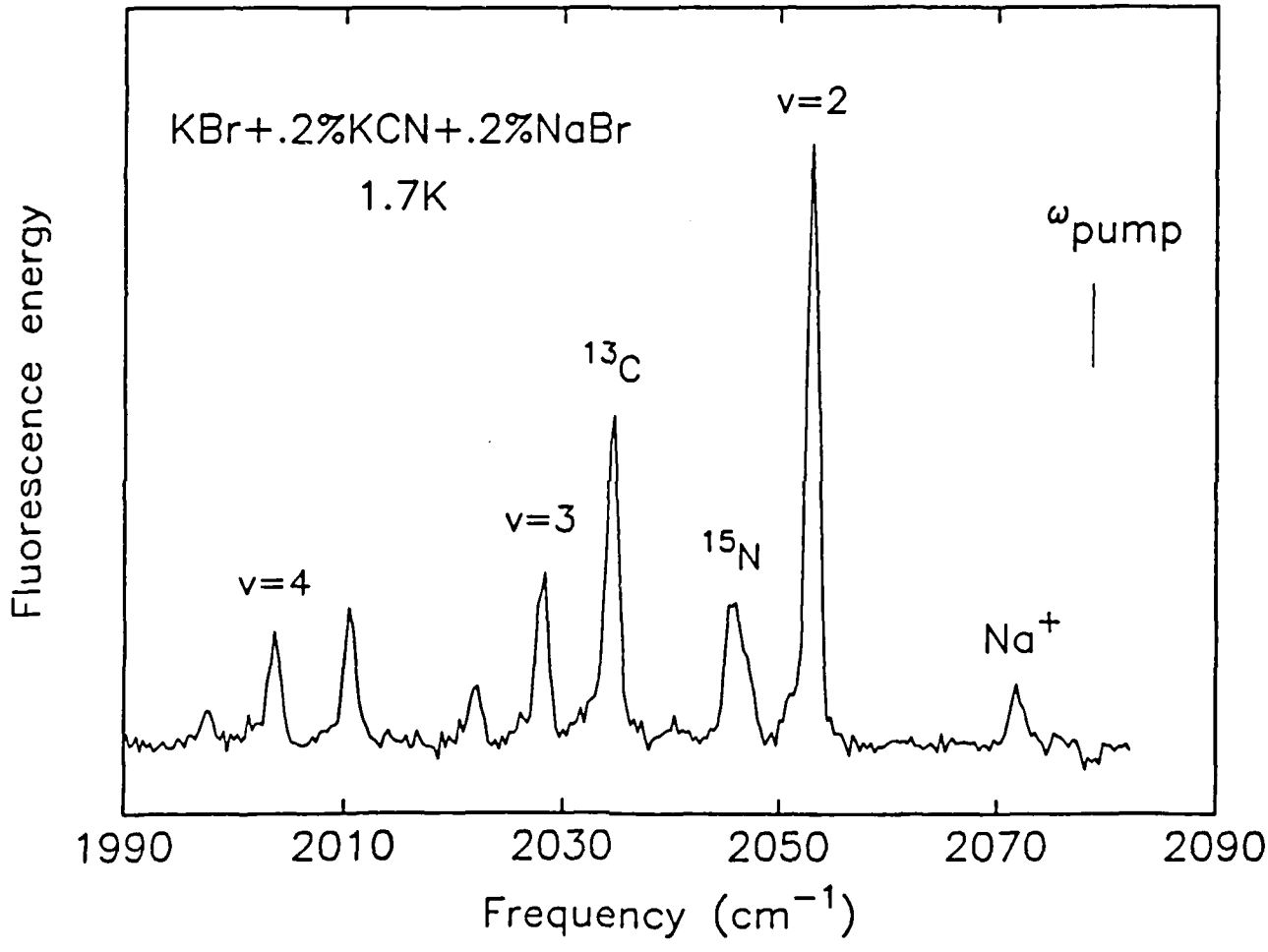

FIG. 16 Vibrational fluorescence of the CN^-:Na^+ center. The CN^- vibrational mode is pumped with the second harmonic of a CO_2 laser. Vibrational fluorescence occurs between higher energy transitions of isolated CN^- and also for the 1→0 transition of the CN^-:Na^+ center.

show a large fluorescence yield because the CN^- excitation energy is tunneled into them. A measurement of the fluorescence life time of this state gives a value about the same as for the isolated CN^-. We conclude that the perturbation produced by the nearby Na^+ ion produces no effect in the vibrational state lifetime.

The presence of the Na^+ neighbor next to the CN^- is observed to produce a very large change in the linewidth or τ_2 time of the CN^- vibrational mode. This unusual effect is most easily seen by examining a spectrum taken at higher temperatures. A spectrum with the sample at 50K is shown in Fig. 17. The spectrum is made up of two types of spectral features: sharp lines and broad bands. The sharp line centered between 2100 and 2125 is due to the C^{13} isotope of NCO^- while the other sharp line at 2071.8 cm^{-1} is due to the CN^-:Na^+ center. The broad band is due to the isolated CN^- molecule. Note that the spectral widths shown in this Figure tell us nothing about the vibrational lifetimes of the molecule since NCO^- does not fluoresce whereas both CN^- and CN^-:Na^+ do with about the same vibrational lifetime. This spectrum demonstrates very clearly that one cannot conclude much about vibrational lifetimes in solids by measuring only the low signal absorption spectrum.

2.3.5 Discovery of the first solid state IR vibrational laser

Low temperature laser oscillation[18] has been observed from pure vibrational levels of CN^- ions doped into KBr and RbI. The lasing in these systems is on the 2→1 vibrational transition but the systems are optically pumped on the 0→1 transition by the second harmonic of a TEA CO_2 laser, Population in the v=2 state occurs through an efficient vibrational energy exchange process[1].

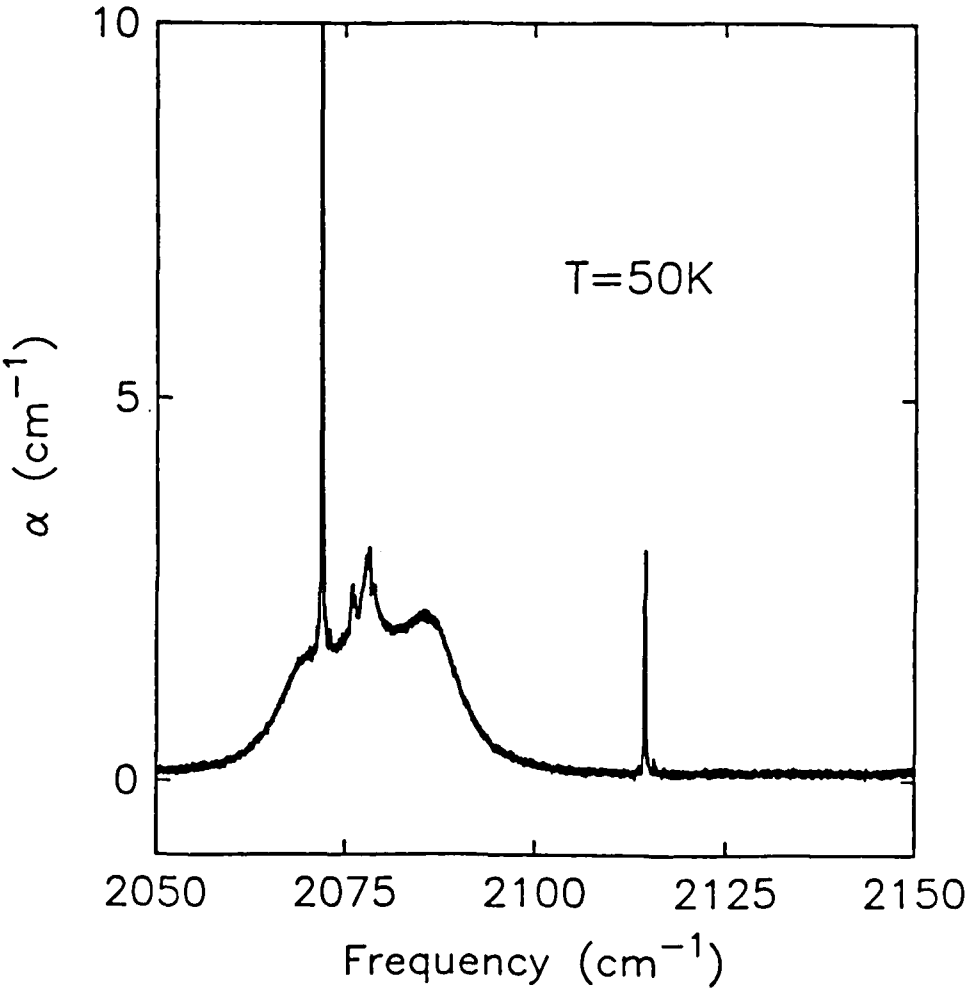

FIG. 17 Impurity induced absorption spectrum of CN^- and $CN^-:Na^+$ at an elevated temperature. The sharpline at 2071.8 cm^{-1} is associated with the $CN^-:Na^+$ center while the 25 cm^{-1} wide line encompassing it is due to isolated CN^-. Both modes have about the same vibrational lifetime.

Samples for these experiments were obtained from Czocralski grown alkali halide boules which were doped with up to 0.5 mole % KCN. During fluorescence experiments, a sample was irradiated with 300μJ, 100 ns pulses produced by second harmonic generation of a TEA CO_2 laser. Radiation emitted from the sample was imaged into a monochromator and detected with an InSb photodiode.

The spectral distribution of the emission was measured in detail with the monochromator for a sample of KBr + 0.5% KCN, which was pumped at 2078.7 cm^{-1}. The fluorescence decay signals were numerically integrated in time to give the total energy emitted at a given frequency following the pump pulse. At 293 K, the broad spectrum shown in Fig. 18a was obtained. The emission lineshape roughly matches the absorption lineshape at this temperature. The large spike at the pump frequency was due to amplifier recovery from the scattered pump radiation. No evidence was found for fluorescence line narrowing.

When the sample temperature was lowered to 1.7 K, however, Fig. 18b shows that the spectrum consisted of a series of bright emission lines, on top of a broad, faint background. Unlike the high temperature case[19], these lines remained unresolved by the monochromator at 0.5 cm^{-1} resolution, and when time resolved displayed a wide variety of rise and decay times.

All of the emission lines in Fig. 18b have been identified and it is instructive to list a few of them here. The pump is at the 0→1 transition of $(^{12}C^{14}N)^-$ and the first line to the red is the 2→1 of the same molecule, the next is the 2→1 of $(^{12}C^{15}N)^-$ and the third, the strongest line in the spectrum, is due to the 1→0 of $(^{13}C^{14}N)^-$. This last result helps pinpoint the important dynamical energy transfer processes. Since this molecule only

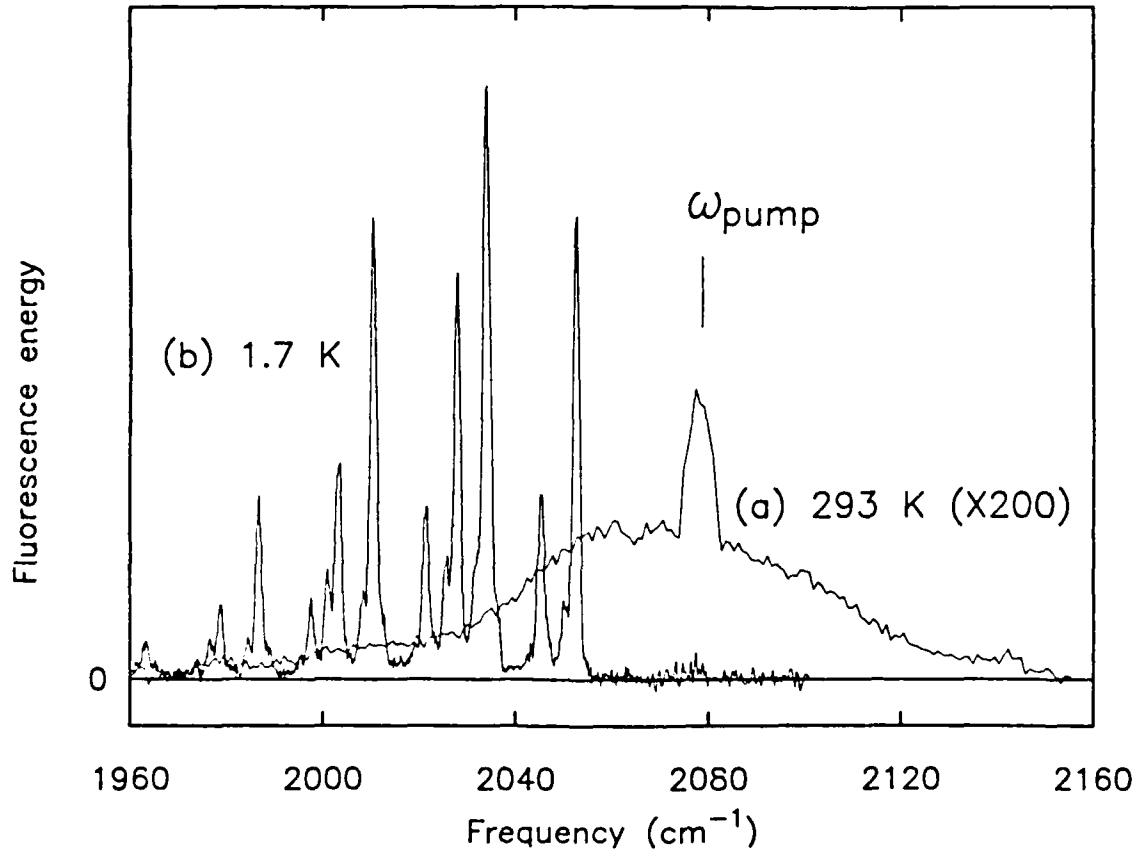

FIG. 18 Fluorescence spectra for the vibrational stretch of CN^- at two temperatures. (a) T = 293K (b) T = 1.7K. The sample is KBr 0.5% KCN. Spectral resolution = 3 cm^{-1}.

accounts for about 1% of the impurities in the crystal, since it is not resonant with the pump radiation and since it has the lowest frequency stretch mode of the three major isotopic combinations, it must function as an energy transfer trap.

A mechanism[18] which accounts for population of upper vibrational levels of anharmonic CN^- oscillators, is diagrammed in Figure 19. Two neighboring oscillators embedded in the host lattice interact via long range dipole-dipole coupling, so that when excited to their v=1 states, they can exchange vibrational quanta. To conserve energy in this 'V-V transfer', a lattice phonon is emitted at a frequency equal to that of the anharmonic shift. This process can efficiently populate ever higher vibrational states through the reaction

$$AB(1) + AB(v) \rightarrow AB(0) + AB(v+1) + \Delta E, \qquad (4)$$

and the isotope shifted states by means of

$$AB(1) + AB_{iso}(v) \rightarrow AB(0) + AB_{iso}(v+1) + \Delta E. \qquad (5)$$

The efficiency of this process is evident in the spectrum shown in Fig. 18 --only a hint remains of the 1→0 fluorescence at the pump frequency. In particular, the intense 2→1 emission at 2054 cm^{-1} indicates population inversion in the v=2 and v=1 levels. To confirm inversion, a measurement of the infrared gain with a diode laser tuned to the 2→1 transition yielded gain coefficients as high as 0.7 cm^{-1}. Larger gain coefficients have been achieved with isotopically pure dopants.

To achieve lasing, resonant cavities were made by cleaving 1mm x 1mm x 5mm doped crystals and evaporating reflective materials directly onto the $1mm^2$ end faces. Gold served as a total reflector on one end while a 1/4 wave

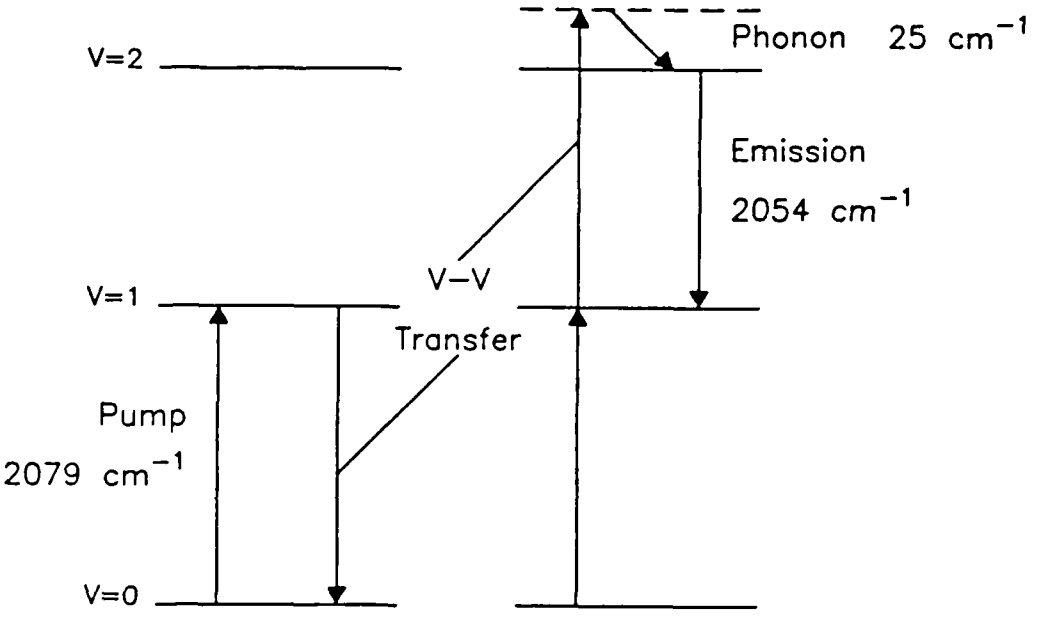

FIG. 19 Energy level diagram for the phonon-assisted V-V transfer process which converts a pair of laser excited v=1 levels to v=2 and v=0 levels. The anharmonic shift is exaggerated for clarity.

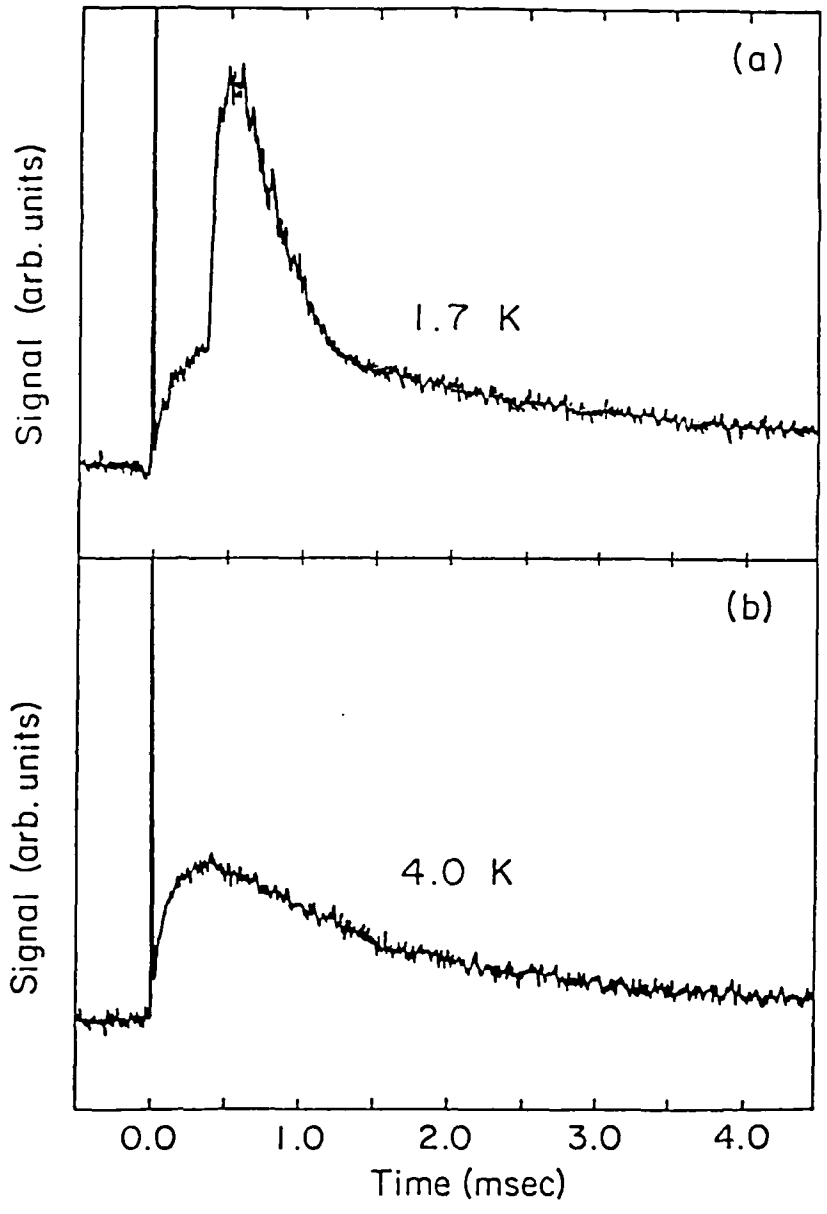

FIG. 20 (a) Single shot example of laser output at 2054 cm^{-1} for a KBr^{+} 0.5% KCN sample at 1.7K. (b) Only the fluorescence background remains with the sample at 4.0K. The spikes at t=o are caused by electrical noise and scattered light.

germanium film on the other served as a 70% reflectivity output coupler. A typical shot with the sample at 1.7 K is shown in Fig. 20. The large peak rising out of the fluorescence background indicates laser oscillation. By comparison, Fig. 20b shows quenching of the gain when the sample temperature was raised to 4.0 K. This resulted from depopulation of the v=2 level through thermal activiation of the reverse of the V-V transfer process described by Eq. 4.

Our experiments on vibrational fluorescence of CN^- in KBr demonstrate that there are two competing cascades for energy transfer among the vibrational levels. The V-V transfer produces a cascade upwards which populates higher levels and the radiative decay produces a cascade downward which depopulates the higher levels. Gas phase analogs of this up-the-ladder cascade of vibrational energy have been observed[20] in low pressure CO and NO, when the translation temperature of the gases were lower than the temperatures of the vibrational populations. In fact, V-V transfer between colliding CO molecules is an important contribution to population inversion of vibration-rotation levels of electric discharge CO lasers.[21] In the gas phase, however, the excess energy due to vibrational anharmonicity is taken up through an increase in the translational energy of the collision partners, while in the solid the excess is taken up by single phonon emission.

Recently, in colaboration with Prof. C. Pollock we have produced continuous wave lasing on the 2→1 vibrational transition of impurity ions in KBr.[22] Population inversion is achieved by optical pumping of the weakly allowed first overtone level of the molecule with a tunable $(F_2^+)_A$ color center laser. A joint grant with Profesor Pollock to develop the CW CN^- laser has been funded.

2.4 Publications (1983-1986)

(Note: An arrow in front of the publication indicates that the work was supported by ARO.)

→ "Observation of Low Temperature Thermal Destabilitzation of Impurity Modes," L. H. Greene and A. J. Sievers, Bull. Amer. Phys Soc. 28, 452 (1983).

→ "Transitory and Persistent IR Spectral Holes in Crystalline Solids Containing Localized Vibrational Modes," A. J. Sievers, Invited Paper at the 7th International Conference on Infrared and Millimeter Waves, Marseille, France (1983).

→ "Spectral Memory" W. E. Moerner, A. R. Chraplyvy and A. J. Sievers, Scientific American April (1983) p. 73-74.

→ "Ultrasonic Modulation of Persistent Spectral Holes in Crystals," H. Lengfellner, T. R. Gosnell, R. W. Tkach and A. J. Sievers, Applied Physics Letters 43, 437 (1983).

"Non-linear IR Properties of an LO Phonon in Thin $KReO_4$ Films," L. H. Greene, Z. Schlesinger and A. J. Sievers, Physical Review B 28, 4863 (1983).

→ "Persistent Nonphotochemical Spectral Hole Dynamics for an Infrared Vibrational Mode in Alkali Halide Crystals," W. E. Moerner, A. R. Chraplyvy, A. J. Sievers and R. H. Silsbee, Phys. Rev. B28 7244 (1983).

"IR Surface Plasmon Spectroscopy," in Ellipsometry and Other Optical Methods for Surface and Thin Film Analysis, F. Abeles ed., Z. Schlesinger and A. J. Sievers, Journal de Physique, Colloque 10, 13 (1983).

"IR Spectroscopy with Surface Electromagnetic Waves," in Dynamics of Interfaces, L. Dobrzynski ed., Z. Schlesinger, Y. J. Chabal and A. J. Sievers, Journal de Physique, Colloque 5, 167 (1984).

→ "Persistent Antiholes in the Vibrational Spectra of Matrix Isolated Molecules," T. R. Gosnell, A. J. Sievers, and R. H. Silsbee, Physical Review Letters 52, 303 (1984).

→ "Matrix-Isolated CN-: A Molecular-Defect Vibrational Laser, T. R. Gosnell, R. W. Tkach and A. J. Sievers, Thirteenth International Quantum Electronics Conference, J. Opt. Soc. Am. B 1, 430 (1984).

→ "Infrared Spectroscopy of $KCl:ND^+_4$," D. M. Kammen, T. R. Gosnell, R. W. Tkach and A. J. Sievers, Bull. Amer. Phys. Soc. 29, 502 (1984).

→ "Infrared Vibrational Fluorescence from Matrix Isolated Molecules at Room Temperature," T. R. Gosnell, R. W. Tkach and A. J. Sievers, Bull. Amer. Phys. Soc. 29, 503 (1984).

→ "Infrared Gain from Vibrational Levels of Matrix Isolated Molecules," R. W. Tkach, T. R. Gosnell and A. J. Sievers, Bull. Amer. Phys. Soc. 29, 503 (1984).

→ "Observation of Two Elastic Configurations at a Point Defect," A. J. Sievers and L. H. Greene, Phys. Rev. Letters 52, 1234 (1984).

→ "Solid State Vibrational Laser-KBr:CN^-," W. Tkach, T. R. Gosnell and A. J. Sievers, Optics Letters 10, 122 (1984).

"Far-Infrared Absorption by Small Metal Particles," R. P. Devaty and A. J. Sievers, Physical Review Letters 52, 1344 (1984).

→ "Anharmonic Vibrational Relaxation Dynamics for a Molecular Impurity Mode in Alkali Halide Crystals,"W. E. Moerner, A. R. Chraplyvy and A. J. Sievers, Physical Review B29, 6694 (1984).

"Enhanced Far Infrared Absorption in $CePd_3$ and $YbCu_2Si_2$, I Experiment," F. E. Pinkerton, M. B. Maple, B. C. Sales and A. J. Sievers, Physical Review B 29, 609 (1984)

→ "Persistent IR Holes and Antiholes in the Vibrational Spectra of Matrix Isolated Molecules," A. J. Sievers, International Conference on Defects in Crystals, Salt Lake City, Utah, August, (1984), p. 422.

→ "Solid State Vibrational Laser-KBr:CN^-," R. W. Tkach, T. R. Gosnell and A. J. Sievers, Optics Letters 10, 122 (1984).

→ "Lasing from a Vibrational Transition of a Molecular Defect," T. R. Gosnell and R. W. Tkach, Journ. of Lumin. 31 & 32 (1984).

→ "Low Temperature Dielectric Properties of KI:Ag^+: Additional Evidence for the coexistence of two elastic configurations," S. B. Hearon and A. J. Sievers, Physical Review B30 4853 (1984).

→ "Matrix-Isolated CN^-: A Molecular-Defect Vibrational Laser," Thirteenth International Quantum Electronics Conference, T. R. Gosnell, R. W. Tkach and A. J. Sievers, J. Opt. Soc. Am B1, 430 (1984).

→ "Spectroscopic Evidence for Two Simultaneous Elastic Configurations at a Point Defect in a Cubic Crystal," A. J. Sievers, L. H. Greene and S. B. Hearon, Ninth International Conference on Infrared and Millimeter Waves, K. Mizuno ed. Japan Society of Applied Physics, (1984) p. 144.

"Anomalous Far Infrared Absorption in Valence Fluctuation Compounds," Ninth International Conference on Infrared and Millimeter Waves Digest, K. Mizuno ed. Japan Society of Applied Physics (1984) p. 446.

"Enhanced Far Infrared Absorption in $CePd_3$ and $YbCu_2Si_2$: Comparison of a Resonant Scattering Model with Experiment," (1984) F. E. Pinkerton, B. C. Webb, J. W. Wilkins, L. J. Sham and A. J. Sievers, Physical Review B30, 3068 (1984).

"Observation of an Index-of-Refraction-Induced Change in the Drude Parameters of Ag Films," Phys. Rev. B30 4189 (1984) with H. Grugger, M. Jurich and J. D. Swalen.

→ "High Temperature Vibrational Fluorescence of CN^- Ions in Alkali Halides," T. R. Gosnell, R. W. Tkach and A. J. Sievers, Solid State Communications 53, 419 (1985).

"The Effect of Melting of the Metallic Component on the Anomalous Far-Infrared Absorption of Superconducting Sn Particle Composites," W. A. Curtin, R. C. Spitzer, N. W. Ashcroft and A. J. Sievers, Phys. Rev. Letters B 31, 2527 (1985).

"Absorptivity of $CePd_3$ from 5 to 400 meV," B. C. Webb, T. Mihalisin and A. J. Sievers, Journal of Applied Physics 57, 3134 (1985).

"Possibility of Observing Quantum Size Effects in the Electromagnetic Absorption Spectrum of Small Metal Particles" R. P. Devaty and A. J. Sievers, Physical Review B32, 1951 (1985).

"Dipole-Dipole-Interaction-Induced Line Narrowing in Thin Film Vibrational Mode Spectra," Z. Schlesinger, L. H. Greene and A. J. Sievers, Physical Review B32, 2721 (1985).

"Spontaneous Emission and Laser Oscillation from Vibrational Levels of Molecular Defects in Solids," T. R. Gosnell, R. W. Tkach and A. J. Sievers, Infrared Physics 25, 35 (1985).

→ "Ultrasonic Attenuation Measurements on Crystals which Display Persistent Nonphotochemical IR Spectral Hole Burning," H. Lengfellner and A. J. Sievers, Phys. Rev. B31, 2591 (1985).

→ "Far-Infrared Properties of Lattice Resonant Modes. VII. Excited States and Paraelectric Pairs," L. H. Greene and A. J. Sievers, Phys. Rev. B31, 3948 (1985).

→ "Persistent Spectral Hole Burning Properties of Na^+-CN^- Pairs in KBr," W. P. Ambrose, R. C. Spitzer, T. R. Gosnell and A. J. Sievers, Bulletin of the Amer. Phys. Soc. 30, 419 (1985).

→ "Sharp Vibrational Lines and Persistent Spectral Holes for Matrix Isolated Molecules," R. C. Spitzer, W. P. Ambrose, T. R. Gosnell and A. J. Sievers, Bulletin of the Amer. Phys. Soc. 30, 643 (1985).

→ "Continuous Wave Operating of the KBr:CN^- Solid State Vibrational Laser in the 5-μm Region," T. R. Gosnell, A. J. Sievers and C. R. Pollock, Optics Letters, 10, 125 (1985).

→ "Bypassing the Manley-Rowe Limit in the KBr:CN^- Vibrational Laser by Energy Recycling," T. R. Gosnell, A. J. Sievers and C. R. Pollock, Bull. Amer. Phys. Soc. 30, 419 (1985).

→ "Influence of Energy Transfer on the CW Operation of the KBr:CN^- Solid State Vibrational Laser," T. R. Gosnell, A. J. Sievers and C. R. Pollock, Conference on Lasers and Electro Optics (1985).

END

DTIC

8-86